Bunsen burner flames at elevated pressures: Lessons from simple chemistry Direct Numerical Simulation analysis

Nilanjan Chakraborty

School of Mechanical and Systems Engineering, Newcastle University, Newcastle Upon Tyne, UK

The 1st International Workshop on Near Limit Flames

29th July, 2017, Boston University, Boston, USA

Acknowledgements

- **Prof. Markus Klein**,Universität der Bundeswehr München, Germany
- **Mr. Heinrich Nachtigal**, Universität der Bundeswehr München, Germany
- **Ms. Dana Alwazzan**, Newcastle University, United Kingdom

Funding & Computing support:

- **EPSRC**
- **N8**
- **ARCHER**
- **Leibnitz Supercomputing Centre**

EPSRC
Engineering and Physical Sciences Research Council

N8 Research Partnership | High Performance Computing

lrz Leibniz-Rechenzentrum der Bayerischen Akademie der Wissenschaften

archer

Outline of the presentation

- Motivation
- Computational challenges
- Objectives
- Mathematical Background
- Numerical implementation & DNS database
- Results & Discussion
- Conclusions

Motivation

- In many engineering applications (e.g. spark ignition engines and industrial gas turbines) turbulent premixed combustion takes places at elevated pressures.
- With the advent of high performance computing CFD plays an increasingly important role for the purpose of optimising combustion processes in internal combustion engines and gas turbines.
- Direct Numerical Simulations (DNS), which resolve all the length and time scales of fluid turbulence without any recourse to physical approximations, are not feasible for the configurations relevant to aforementioned engineering applications. Most industrial calculations are done using Reynolds-Averaged Navier Stokes (RANS) and Large Eddy Simulations (LES) which need combustion models.
- Most combustion models are derived and validated only for atmospheric pressure. Therefore it is crucial to assess if these models are valid for elevated pressure conditions.

Challenges for high pressure simulations (1)

- The laminar burning velocity for hydrocarbon-air (e.g. methane-air) mixtures often scales as: $\boldsymbol{S_L \sim S_L^0 (p/p_0)^{-0.5}}$.

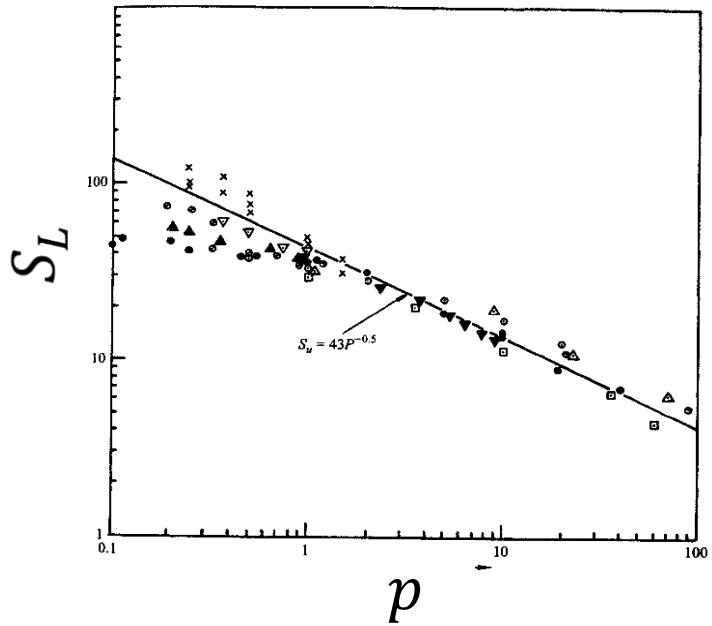

Taken from: "An introduction to combustion, Concepts and Applications" by S.R. Turns

- This suggests that for a given rms velocity fluctuation the velocity ratio u'/S_L scales as: $\boldsymbol{u'/S_L \sim (p/p_0)^{0.5}}$

Challenges for high pressure simulations (2)

- For isobaric combustion of ideal gases: $\rho \sim p$ and thus the kinematic viscosity ν scales as: $\boldsymbol{\nu \sim p^{-1}}$.

- Thus the flame thickness scales as: $\boldsymbol{\delta_{th} \sim \nu / S_L \sim p^{-1/2}}$. Thus integral length scale to flame thickness ratio l/δ_{th} scales as: $\boldsymbol{l/\delta_{th} \sim p^{0.5}}$.

- As a result, the turbulent Reynolds number for a given burner with a given set of values of rms turbulent velocity fluctuation u' and integral length scale l scales as:

$$\boldsymbol{Re_t = \frac{u'l}{\nu} \sim \frac{u'l}{S_L \delta_{th}} \sim p}$$

Objectives

- To analyse the scalar gradient (or flame thickness) and curvature statistics with an increase in pressure for Bunsen burner configuration
- To assess if a high pressure flame behaves in the same manner (in terms of above statistics) as that of a flame with same turbulent Reynolds number but at a lower pressure

- It is recognised that a change in pressure for a given flow condition for a burner means the flames are at different locations on the combustion regime diagram.
- The present analysis focuses only on fluid-dynamical aspects of pressure variation.

Mathematical Background

The generic chemical reaction for premixed flames can be written as:

$$Reactants \rightarrow Products$$

It is possible to define a reaction progress variable c which increases monotonically from 0 to 1 from fresh reactants to completely burned products

$$c = \frac{Y_{R0} - Y_R}{Y_{R0} - Y_{R\infty}} \quad ;$$

Subscript 0: unburned gas value
Subscript ∞: burned gas value

Transport equation of reaction progress variable (c):

$$\rho \frac{\partial c}{\partial t} + \rho u_k \frac{\partial c}{\partial x_k} = \frac{\partial}{\partial x_k}\left(\rho D \frac{\partial c}{\partial x_k}\right) + \dot{w}$$

The above equation can be written in kinematic form as:

$$\frac{\partial c}{\partial t} + u_j \frac{\partial c}{\partial x_j} = \boxed{(S_d)}\left|\nabla c\right| \Rightarrow S_d = \left[\frac{\dot{w} + \nabla.(\rho D \nabla c)}{\rho \left|\nabla c\right|}\right]$$

Displacement speed

Deformation & stretching of premixed flames

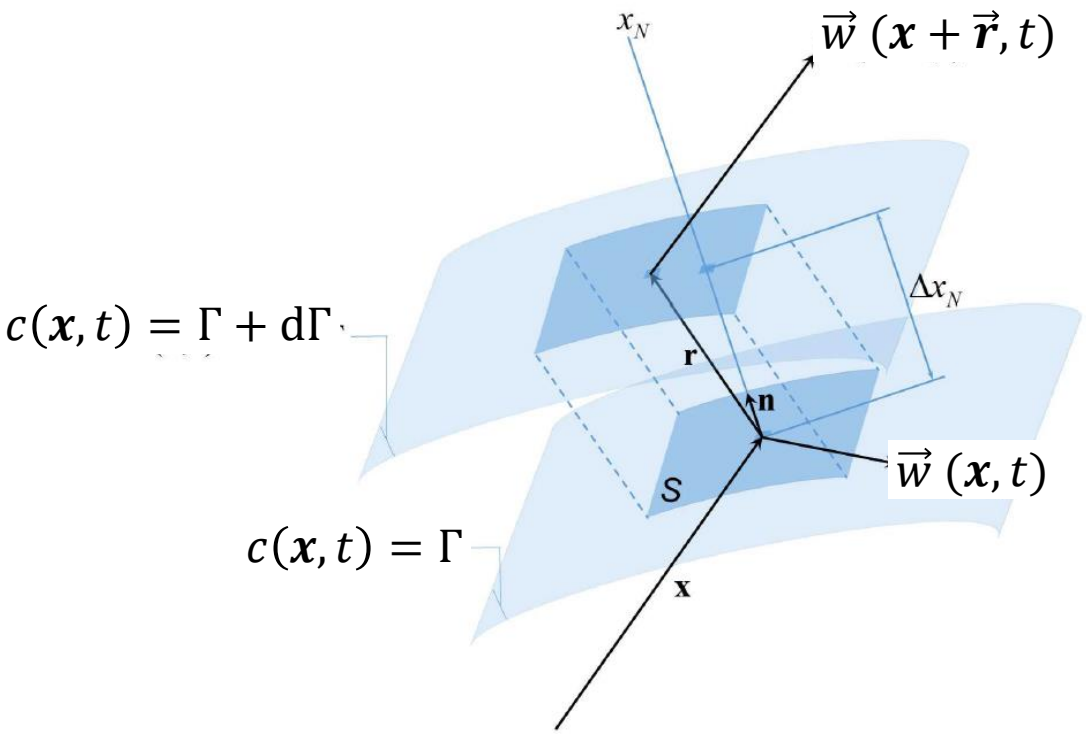

$$\frac{d\vec{r}}{dt}=\vec{r}.\nabla\vec{w} \quad \Rightarrow \quad \frac{dr_i}{dt}=r_j\frac{\partial w_i}{\partial x_j}$$

Here $\dfrac{d}{dt}=\dfrac{\partial}{\partial t}+\vec{w}.\nabla$

Deformation & stretching (1)

- The transport equation of c takes the following form:

$$\frac{\partial(\rho c)}{\partial t}+\frac{\partial(\rho u_j c)}{\partial x_j}=\frac{\partial}{\partial x_j}\left(\rho D\frac{\partial c}{\partial x_j}\right)+\dot{w} \quad (1)$$

Reaction rate

Molecular diffusion rate

- For a given c –isosurface the above equation can be recast in kinematic form in the following manner:

$$\frac{dc}{dt}=\frac{\partial c}{\partial t}+\vec{w}\cdot\nabla c=\frac{\partial c}{\partial t}+w_j\frac{\partial c}{\partial x_j}=0 \quad (2)$$

- Here $\vec{w}$ is the propagation velocity and a comparison between Eqs. (1) and (2) suggest that

$$w_j=u_j+\underbrace{\left[\frac{\dot{w}+\nabla.(\rho D\nabla c)}{\rho|\nabla c|}\right]}_{S_d}N_j$$

Deformation & stretching (2)

- A surface A (t) is considered to be moving in space with an arbitrary velocity $\vec{w}$. The surface is bounded by a circuit C (t) and its normal vector is $\vec{N}$. The velocity field $\vec{w}$ is assumed to be prescribed over a domain swept by the moving surface A (t). Under these assumptions the rate of change of flux of a vector across the surface A (t) is given by:

$$\frac{d}{dt}\int_{A(t)} \vec{G}.\vec{N}dA = \int_{A(t)} \left[\frac{\partial \vec{G}}{\partial t} + \vec{w}.\nabla\vec{G} - \vec{G}.\nabla\vec{w} + \vec{G}\nabla.\vec{w} \right].\vec{N}dA = \int_{A(t)} \left[\frac{\partial G_i}{\partial t} + w_j \frac{\partial G_i}{\partial x_j} - G_j \frac{\partial w_i}{\partial x_j} + G_i \frac{\partial w_j}{\partial x_j} \right] N_i dA$$

$$\vec{G} = \vec{N}$$

Stretch rate:

$$\boxed{\frac{1}{\delta A}\frac{d(\delta A)}{dt} = (\delta_{ij} - N_i N_j)\frac{\partial w_i}{\partial x_j} = (\delta_{ij} - N_i N_j)\frac{\partial u_i}{\partial x_j} + S_d \frac{\partial N_j}{\partial x_j} = a_T + 2S_d \kappa_m}$$

Tangential strain rate: $a_T = (\delta_{ij} - N_i N_j)\dfrac{\partial u_i}{\partial x_j}$

Stretch/Effective tangential strain rate: $a_T^{eff} = (\delta_{ij} - N_i N_j)\dfrac{\partial w_i}{\partial x_j} = a_T + 2S_d \kappa_m$

Mean curvature (i.e. mean of principal curvatures): $\kappa_m = (\kappa_1 + \kappa_2)/2 = 0.5\nabla.\vec{N}$

Pope (1988) ; Dopazo et al. (2015)

Deformation & stretching (3)

- The kinematic equation of reaction progress variable can be recast as:

$$\frac{\partial c}{\partial t} + w_j \frac{\partial c}{\partial x_j} = 0 \Rightarrow \frac{\partial c}{\partial t} + u_j \frac{\partial c}{\partial x_j} + S_d N_j \frac{\partial c}{\partial x_j} = 0 \Rightarrow \frac{\partial c}{\partial t} + u_j \frac{\partial c}{\partial x_j} = S_d |\nabla c|$$

- Taking gradient of the final equation as:

$$\frac{d|\nabla c|}{dt} = \left[\frac{\partial |\nabla c|}{\partial t} + w_j \frac{\partial |\nabla c|}{\partial x_j} \right] = -\left[N_j N_k \frac{\partial u_j}{\partial x_k} + N_k \frac{\partial S_d}{\partial x_k} \right] |\nabla c| = -N_j N_k \frac{\partial w_j}{\partial x_k} |\nabla c|$$

Effective normal strain rate : $\boxed{a_N^{eff} = N_j N_k \frac{\partial w_j}{\partial x_k} = N_j N_k \frac{\partial u_j}{\partial x_k} + N_k \frac{\partial S_d}{\partial x_k}}$

Normal strain rate : $\boxed{a_N = N_j N_k \frac{\partial u_j}{\partial x_k}}$ **Additional strain rate due to propagation:** $\boxed{N_k \frac{\partial S_d}{\partial x_k}}$

- Let us now consider these relations:

$$\boxed{\frac{1}{\Delta x_N} \frac{d\Delta x_N}{dt} = \left[N_j N_k \frac{\partial u_j}{\partial x_k} + N_k \frac{\partial S_d}{\partial x_k} \right] = a_N^{eff}} \quad \boxed{\frac{1}{|\nabla c|} \frac{d|\nabla c|}{dt} = -\left[N_j N_k \frac{\partial u_j}{\partial x_k} + N_k \frac{\partial S_d}{\partial x_k} \right] = -a_N^{eff}}$$

Pope (1988) ; Dopazo et al. (2015)

Numerical Implementation

- 3D compressible DNS with single step irreversible Arrhenius type chemistry carried out using a well-known code SENGA (Jenkins & Cant, 1999).
- Outflow boundary conditions are specified using NSCBC technique (Poinsot & Lele, 1992).
- High order finite difference (10th order central difference scheme at the internal grid points and gradually dropping to 2nd order one-sided scheme at non-periodic boundaries and 3rd order explicit Runge-Kutta scheme have been used spatial discretisation and explicit time advancement respectively.
- Standard values are chosen for Prandtl number = 0.7 and Zel'dovich number = 6.0. Lewis number is taken to be unity. These values are representative of stoichiometric methane-air combustion.
- The flame is initialised as:

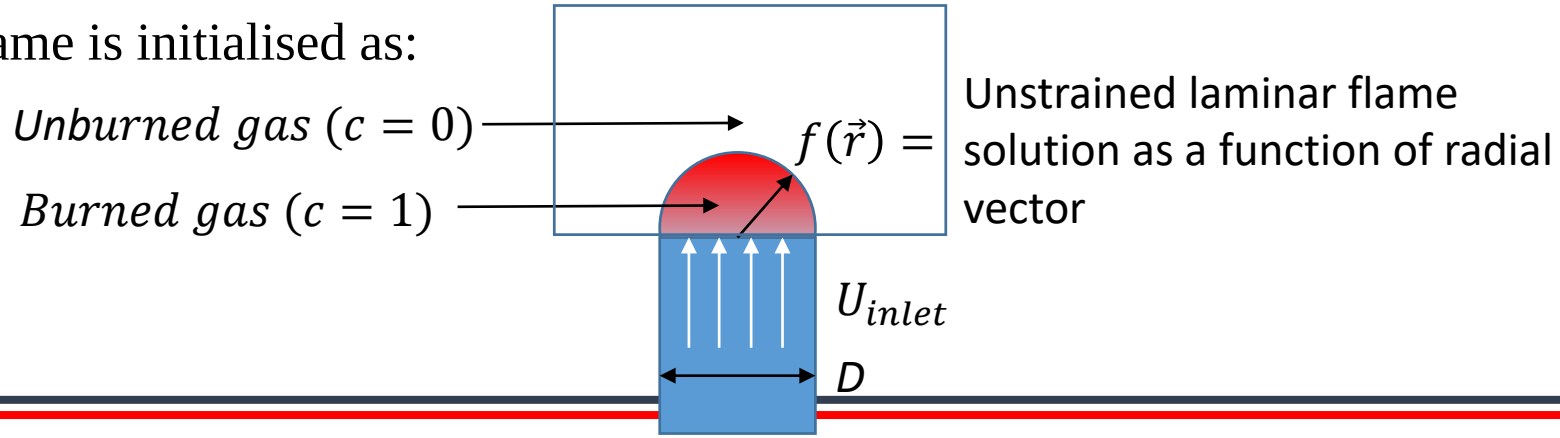

Inflow Boundary condition specification (1)

- Synthetic inlet turbulence is generated by digital filtering random data following Klein et al. (JCP, 186, 2003)

- For a 1D example:
  - r_n be random numbers with $\langle r_n \rangle = 0,\ \langle r_n^2 \rangle = 1$
  - $b_k,\ k = -N \ldots N$ be the filter coefficients: $b_k = \widetilde{b_k}/B$, B is a normalization factor and $\widetilde{b_k} = \exp(-\pi k^2/2n^2)$
  - $u_m = \sum_{n=-N}^{N} b_n \cdot r_{m+n}$ is a correlated signal with length scale $N \cdot \Delta x$

- Besides the length scale, first and second order one point statistics can be prescribed

Inflow Boundary condition specification (2)

- In this method the filter size is proportional to the desired turbulent length (time) scale divided by Δx (Δt)
- If the filter has a 1D size of N, generation of inlet data for one cell in the inlet plane is an $O(N^3)$ operation.
- This method has been applied successfully to a large number of flow problems
- However, direct application to large scale problems can be inefficient

Inflow Boundary condition specification (3)

The digital filter method can be tuned for high parallel performance in 4 steps

1. The Gaussian filter in time direction has been replaced by an autoregressive AR1 process to avoid excessive filter length (due to small Δt in the compressible solver)

2. The 2D filter in the inlet plane can be replaced by the tensor product of two 1D filters. This replaces the $O(N^2)$ by an $O(N)$ operation

Inflow Boundary condition specification (4)

3. The filtering makes use of all available processors not only those located at the inflow plane

4. Transferring random data before filtering can be avoided by assigning a local unique random seed at start of simulation in overlapping regions.

For more details refer to Klein et al. (JCP, 186, 2003) and Kempf et al. (C&F, 60, 2012), Nachtigal (2017).

Simulation and flow parameters (1)

Case	P/P_0	U_{inlet}/S_L	u'_{inlet}/S_L	L_{11}/D	L_{domain}/D	N_x
A	1.0	6.0	1.0	0.2	2.0	250
B	5.0	6.0	1.0	0.2	2.0	560
C	10.0	6.0	1.0	0.2	2.0	795

- $P_0 = 1.0\ bar$ and statistics are taken after at least 2-throughpass times

Case	P/P_0	Re_D	Re_t	Da	Ka	τ
A	1.0	399.0	13.3	5.00	0.45	4.5
B	5.0	892.0	29.26	11. 36	0.30	4.5
C	10.0	1262.0	41.22	16.13	0.25	4.5

- $Re_D = \frac{\rho_0 U_{inlet} D}{\mu_0}$; $Re_t = \frac{\rho_0 u'_{inlet} L_{11}}{\mu_0}$; $Da = \frac{S_L L_{11}}{u'_{inlet}\delta_{th}}$; $Ka = \left(\frac{u'_{inlet}}{S_L}\right)^{1.5}\left(\frac{L_{11}}{\delta_{th}}\right)^{-0.5}$; $\delta_{th} = (T_{ad} - T_0)/\max|\nabla T|_L$ & $\tau = (T_{ad} - T_0)/T_0$

Flame morphology (1)

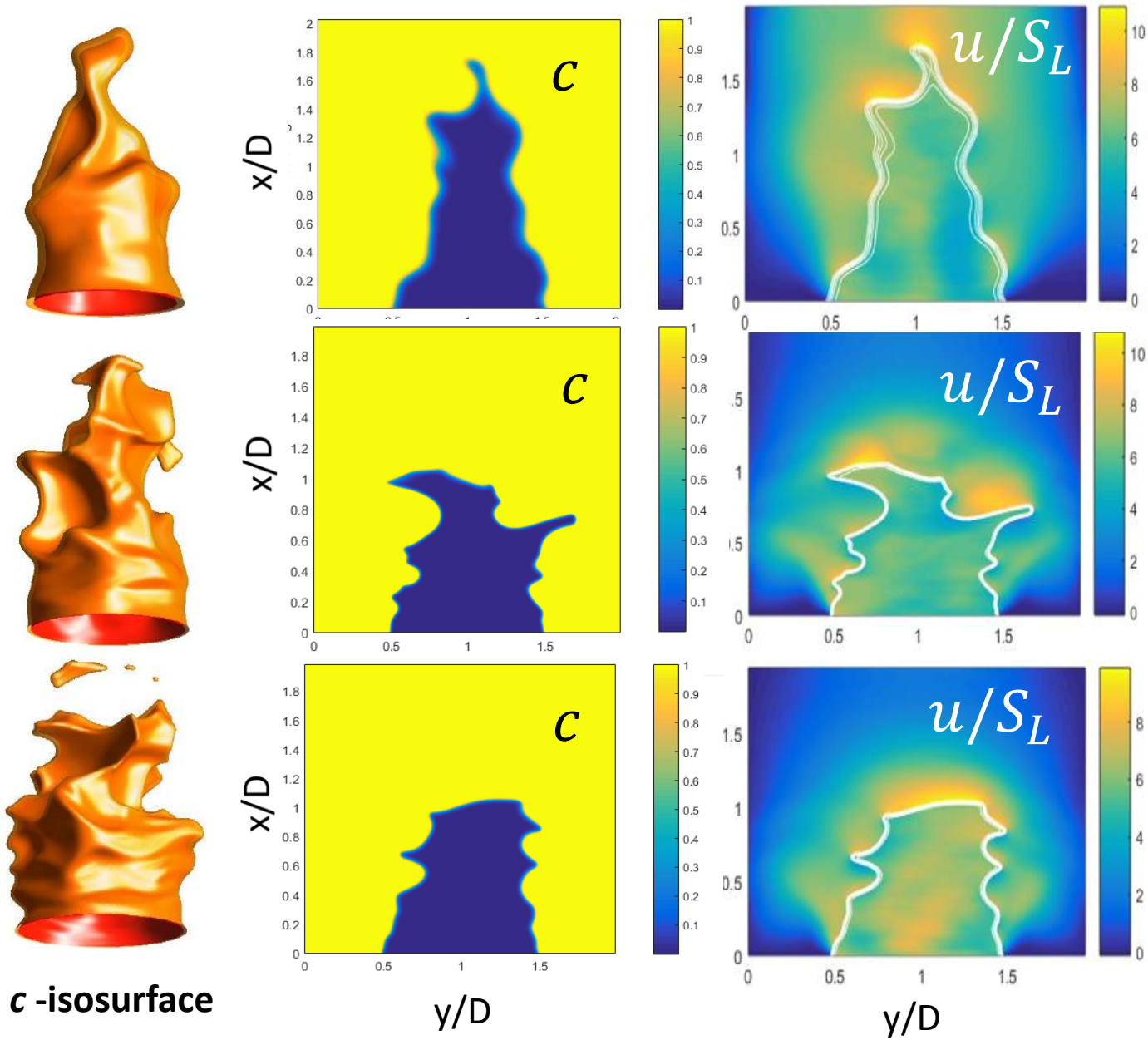

c -isosurface

Case A
(p =p_0)

Case B
(p =5p_0)

Case C
(p =10p_0)

Simulation and flow parameters (2)

Case	P/P_0	U_{inlet}/S_L	u'_{inlet}/S_L	L_{11}/D	L_{domain}/D	N_x
C	10.0	6.0	1.0	0.2	2.0	795
D	1.0	6.0	3.1	0.2	2.0	795
E	1.0	6.0	1.0	0.6	2.0	795

- $P_0 = 1.0\ bar$ and statistics are taken after at least 2-throughpass times

Case	P/P_0	Re_D	Re_t	Da	Ka	τ
C	10.0	1262.0	41.22	16.13	0.25	4.5
D	1.0	399.0	41.22	1.61	2.40	4.5
E	1.0	399.0	41.22	16.13	0.25	4.5

- $Re_D = \frac{\rho_0 U_{inlet} D}{\mu_0}$; $Re_t = \frac{\rho_0 u'_{inlet} L_{11}}{\mu_0}$; $\mathrm{Da} = \frac{S_L L_{11}}{u'_{inlet}\delta_{th}}$; $\mathrm{Ka} = \left(\frac{u'_{inlet}}{S_L}\right)^{1.5}\left(\frac{L_{11}}{\delta_{th}}\right)^{-0.5}$;

$\delta_{th} = (T_{ad} - T_0)/\max|\nabla T|_L$ & $\tau = (T_{ad} - T_0)/T_0$

Flame morphology (2)

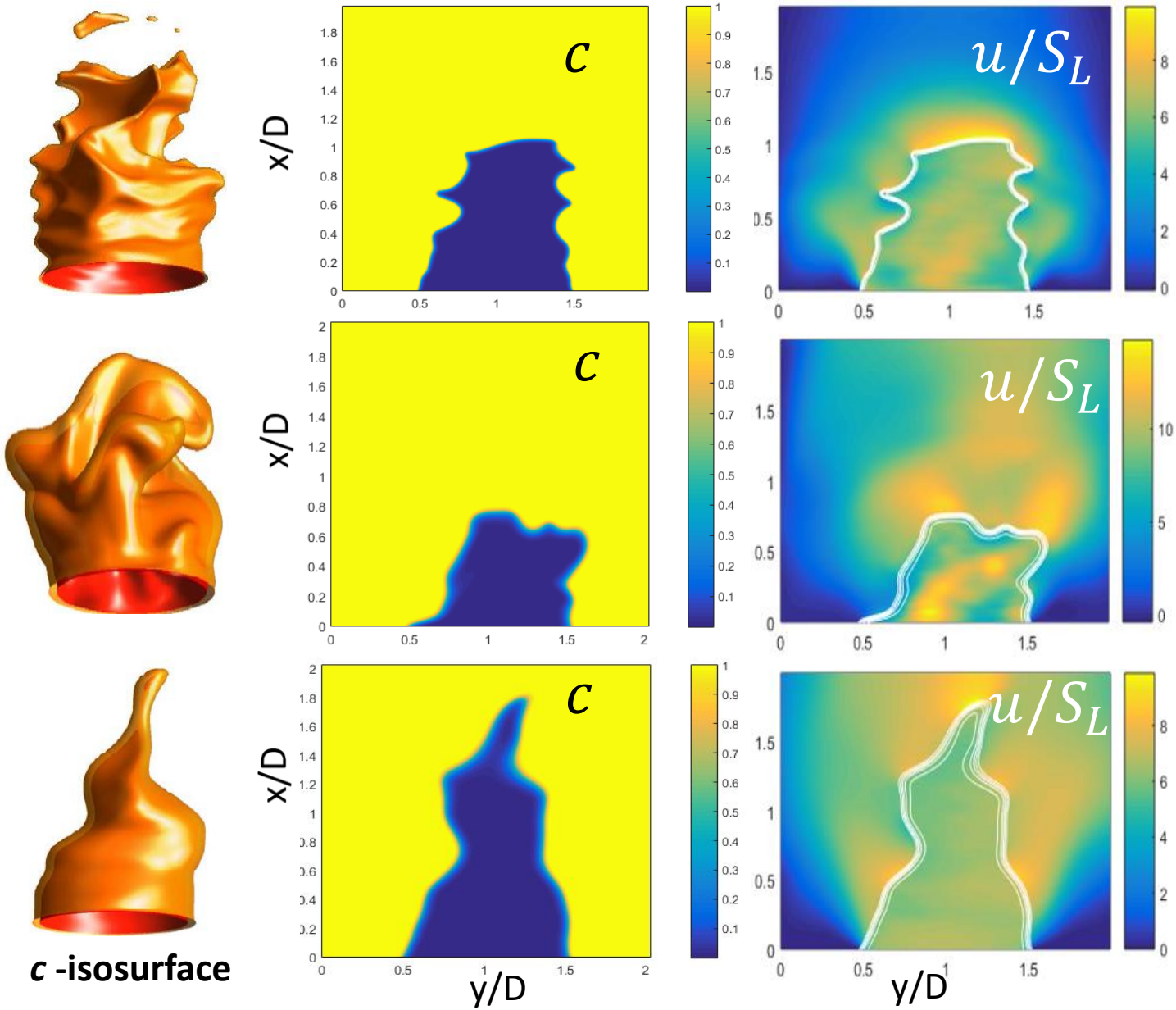

c -isosurface

Case C

$(u'_{inlet})/S_L = 1$

$L_{11}/\delta_{th} = 16.13$

$Re_t = 41.22$

$Re_D = 1262.0$

$p = 10p_0$

Case D

$(u'_{inlet})/S_L = 3.1$

$L_{11}/\delta_{th} = 5.20$

$Re_t = 41.22$

$Re_D = 399.0$

$p = p_0$

Case E

$(u'_{inlet})/S_L = 1$

$L_{11}/\delta_{th} = 16.13$

$Re_t = 41.22$

$Re_D = 399.0$

$p = p_0$

Regime diagram locations

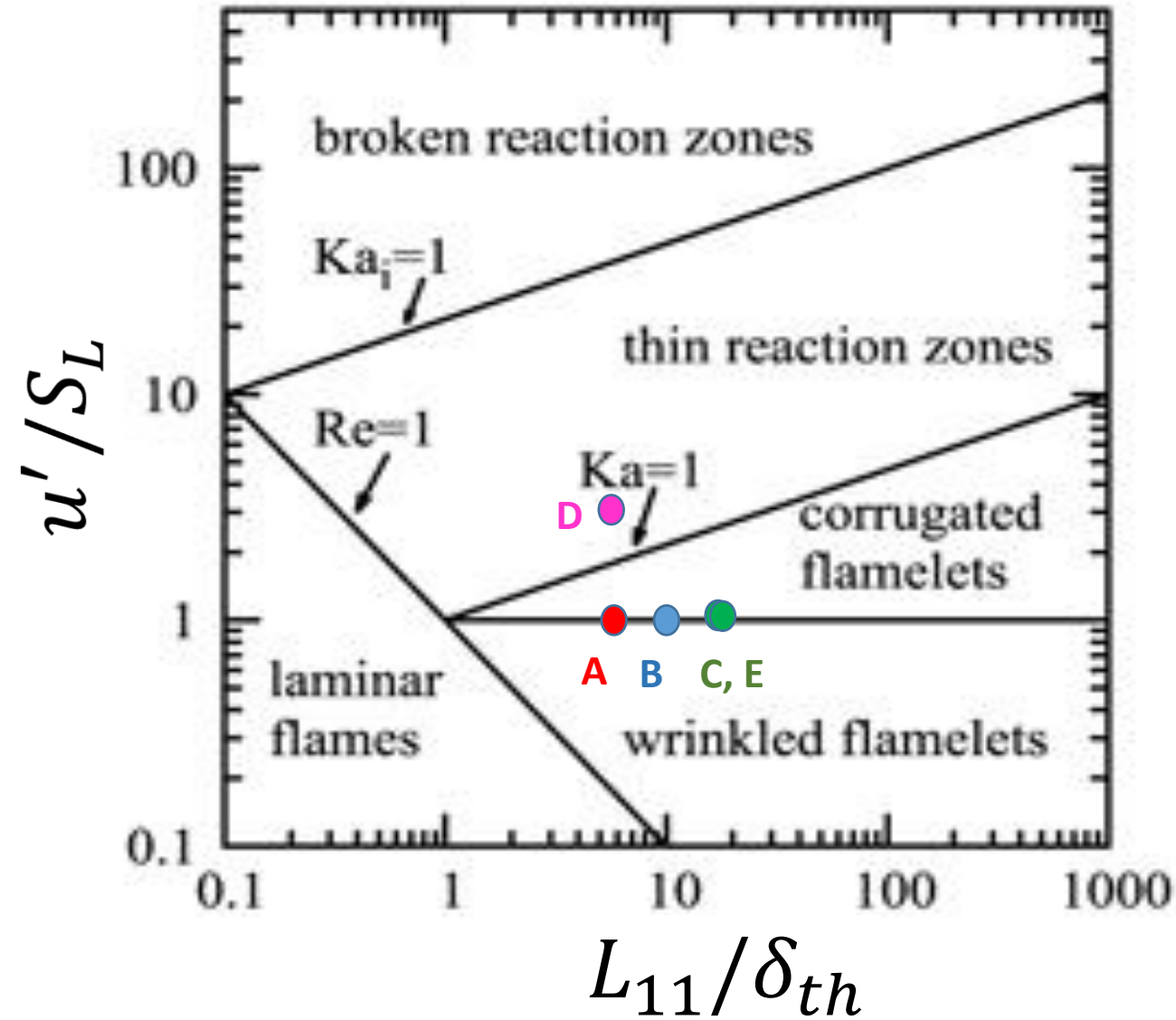

Statistics of $|\nabla c| \times \delta_{th}$: normalised flame thickness

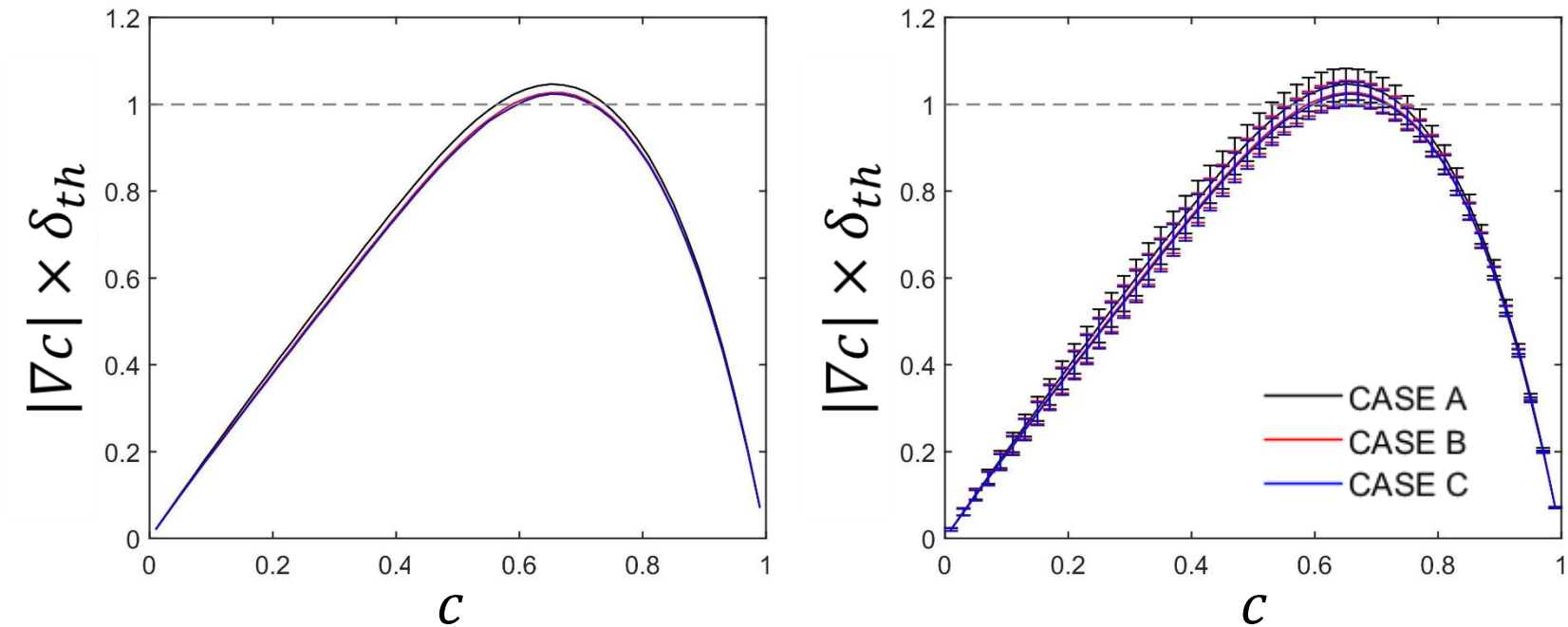

- The quantity $|\nabla c|$ scales as: $|\nabla c| \sim 1/\delta$ where δ is the flame thickness and thus the quantity $|\nabla c| \times \delta_{th} \sim \delta_{th}/\delta$ can be taken to be a measure of the ratio of laminar flame thickness to turbulent flame thickness. Here we can see a small amount of flame thinning under turbulence.
- The standard deviations are shown as bars. Clearly the uncertainly in the difference in the mean value is not significant to draw any meaningful conclusion.
- **No major pressure dependence on the normalised flame thickness.**

Statistics of $|\nabla c| \times \delta_{th}$: normalised flame thickness

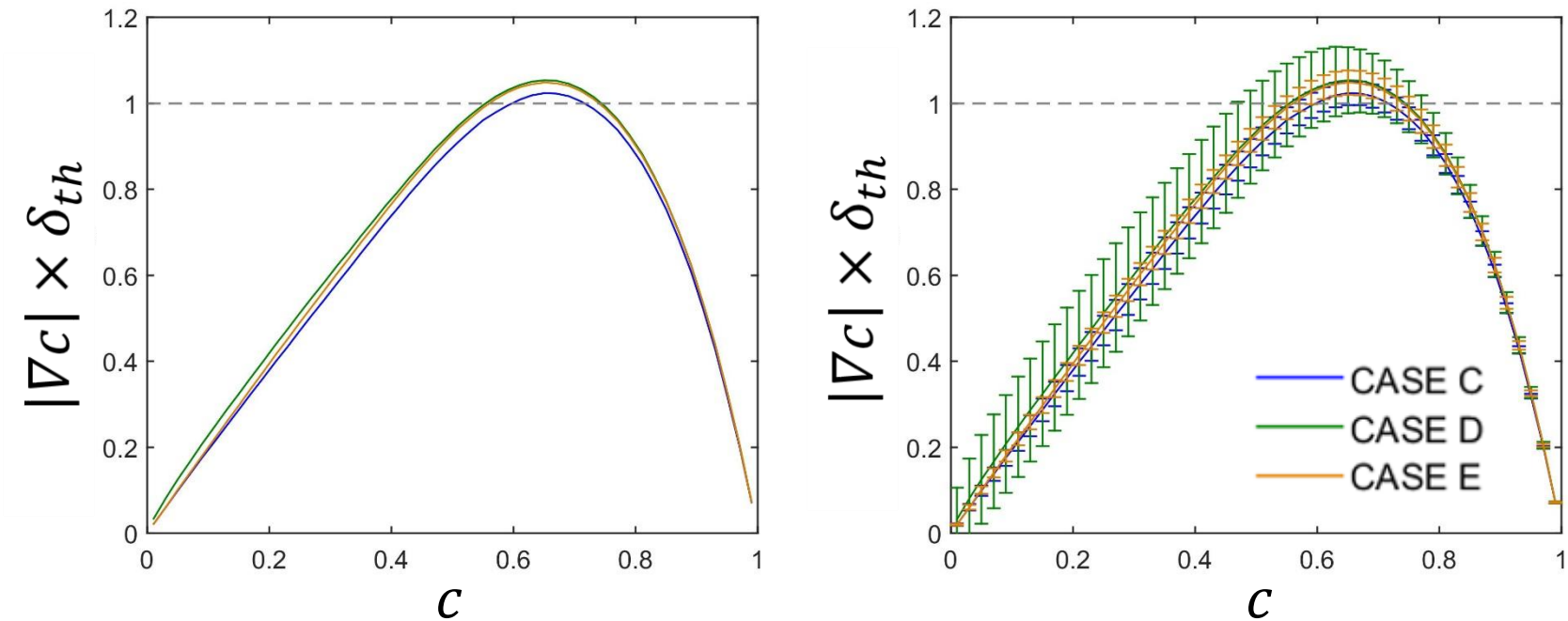

- The standard deviations are shown as bars. Clearly the uncertainly in the difference in the mean value is not significant to draw any meaningful conclusion. Standard deviation increases with increasing u'/S_L.
- **No major u'/S_L and L_{11}/δ_{th} dependences on the mean normalised flame thickness within this parameter range.**

Statistics of $a_N \times \delta_{th}/S_L$: normalised normal strain rate

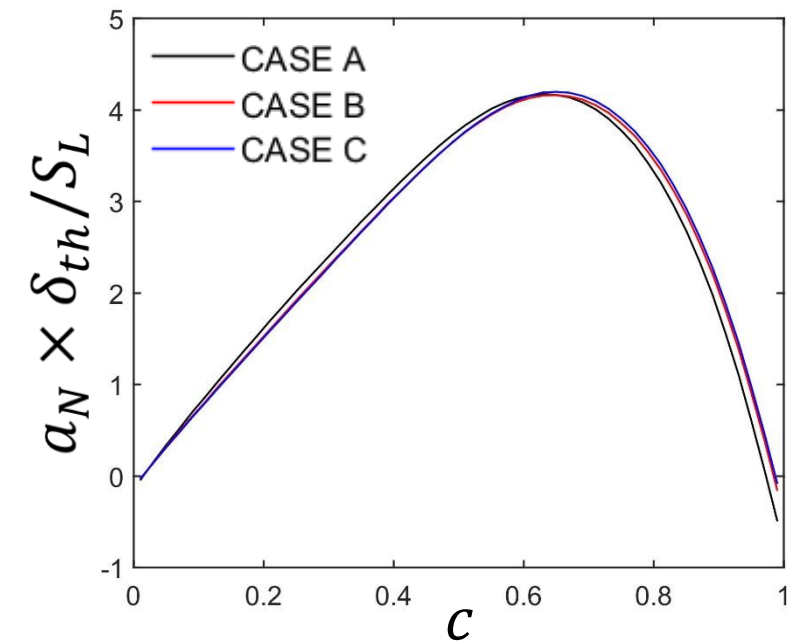

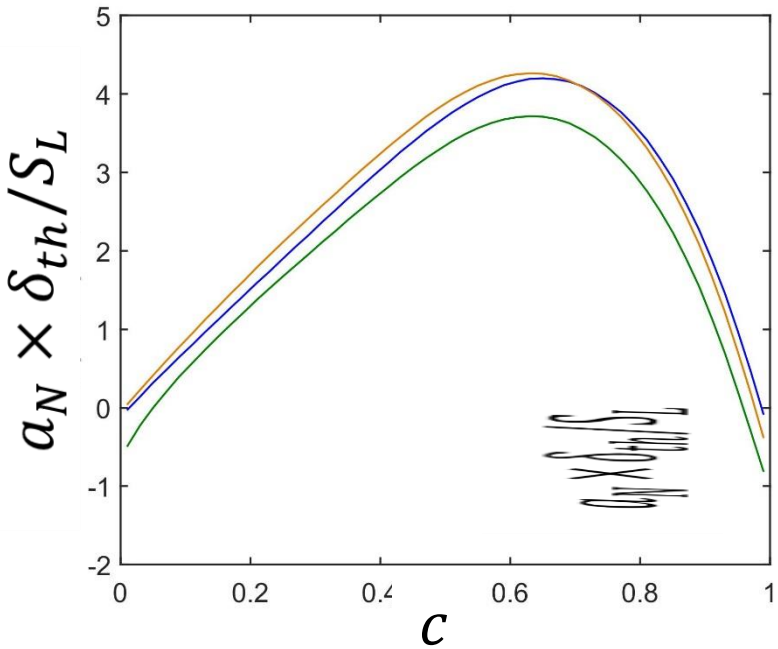

$$\boldsymbol{a_N = (e_\alpha \cos^2 \alpha + e_\beta \cos^2 \beta + e_\gamma \cos^2 \gamma)}$$

- No major pressure dependence on the mean normalised fluid-dynamic normal strain rate.
- No major u'/S_L and L_{11}/δ_{th} dependences on the mean normalised fluid-dynamic normal strain rate within this parameter range.

Statistics of $\nabla.\vec{u} \times \delta_{th}/S_L$: normalised dilatation rate

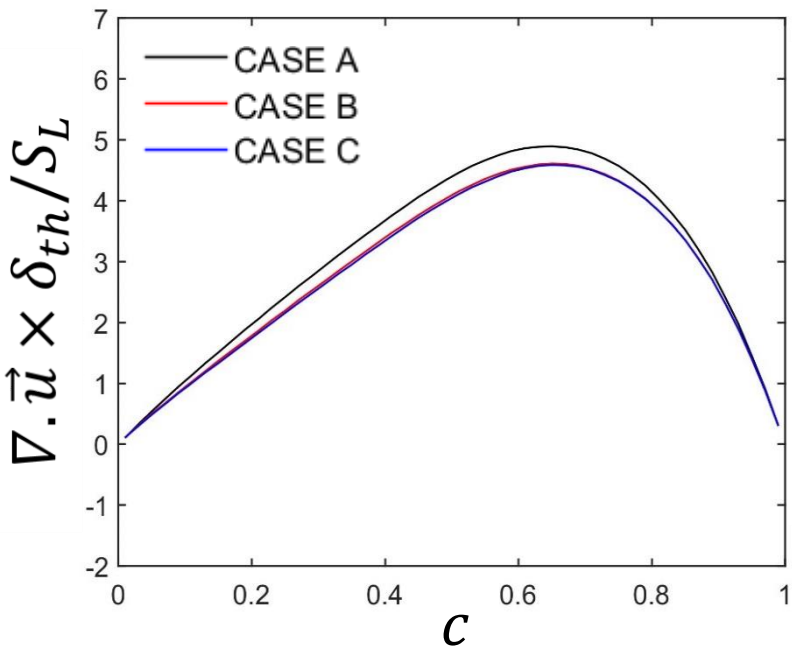

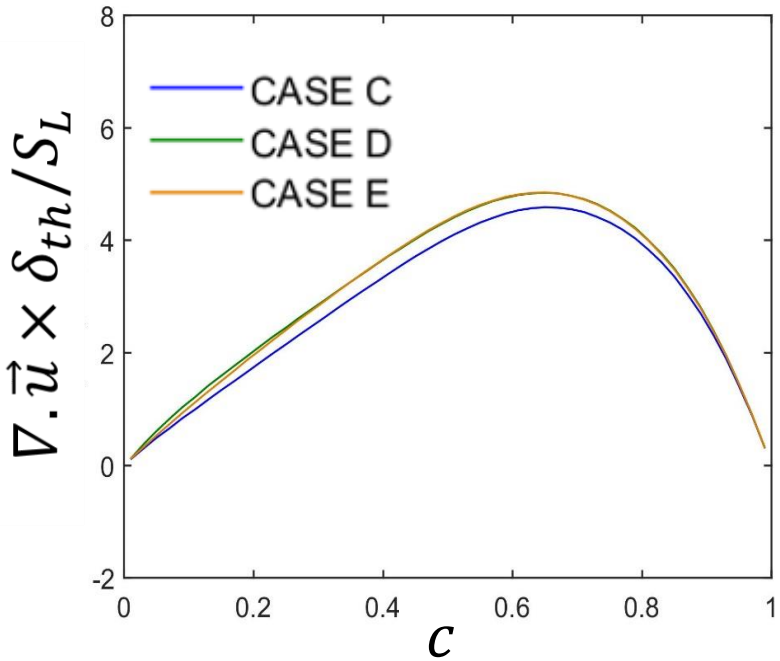

- Case A shows higher mean dilatation rate in comparison to Cases B and C.
- Case E shows higher mean dilatation rate in comparison to Cases C and D.
- Difference in mean dilatation rate warrant further explanation

$a_T \times \delta_{th}/S_L$: normalised tangential strain rate

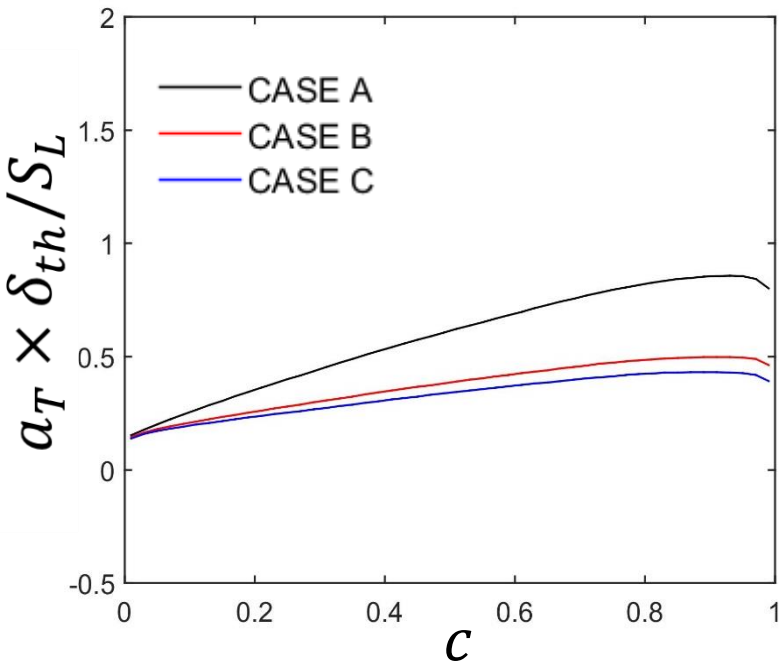

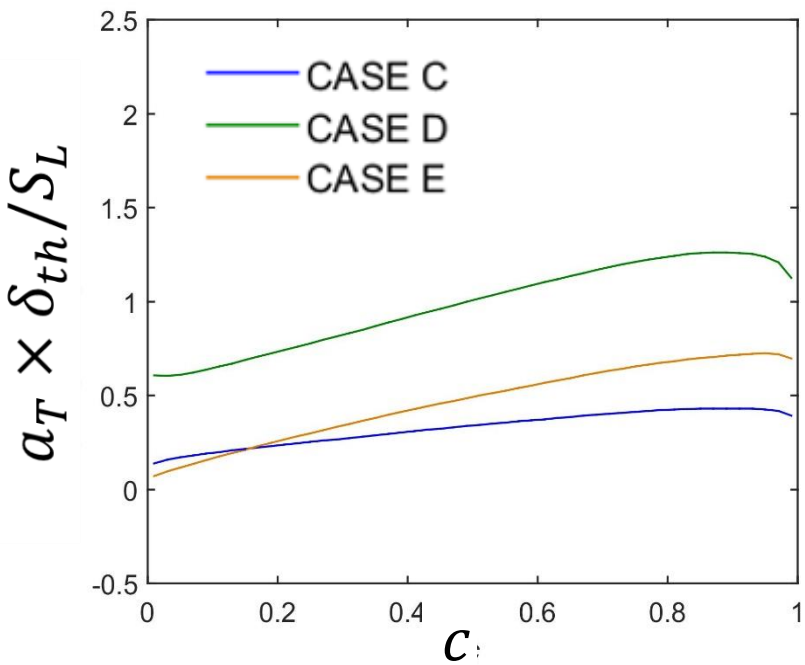

- The mean behaviour of normalised fluid-dynamic tangential strain rate shows some difference.
- The difference in mean tangential strain rate (i.e. $a_{\mathrm{T}} = \nabla.\vec{u} - a_N$) behaviour originates due to the difference in mean values of dilatation rate and normal strain rate

Curvature PDFs (1)

Case A $L_{11}/\delta_{th} = 5$

Case B $L_{11}/\delta_{th} = 11.36$

Case C $L_{11}/\delta_{th} = 16.13$

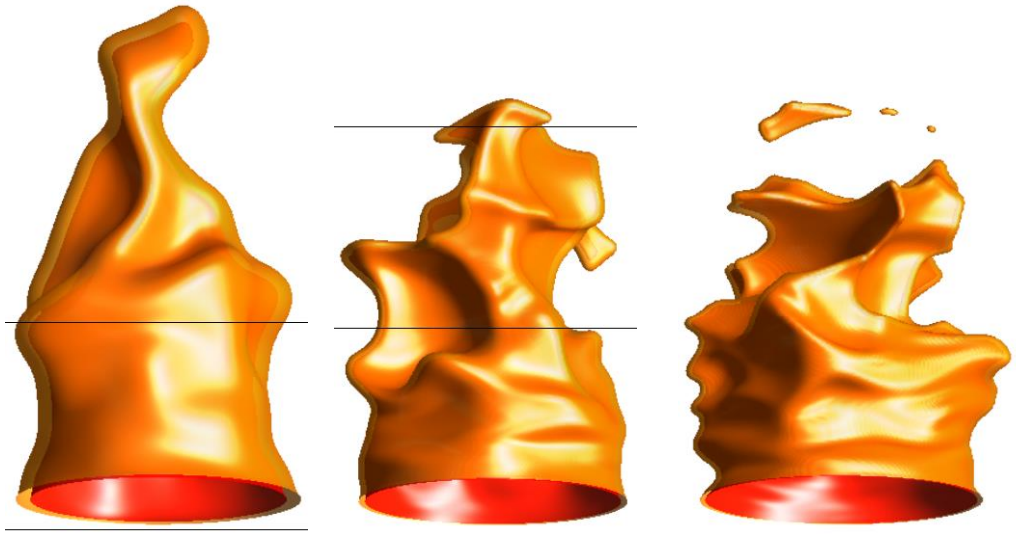

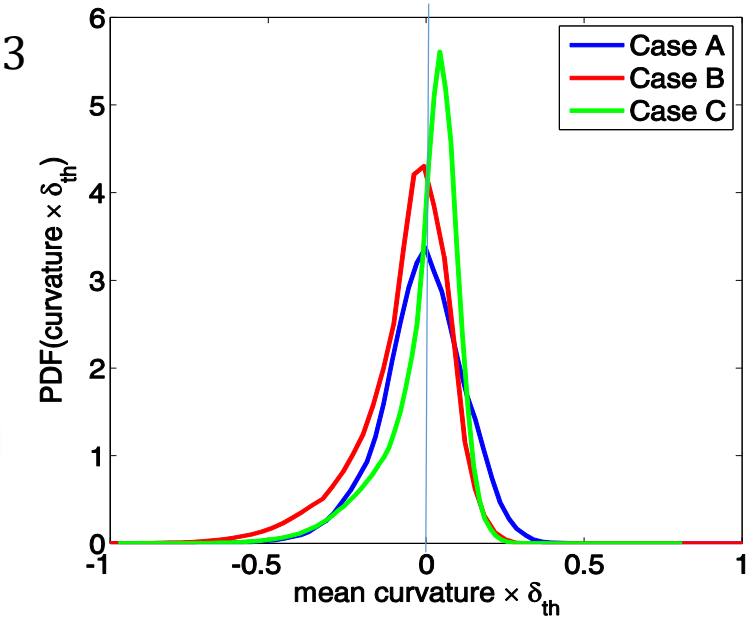

- Curvature PDFs for cases A-C. Mean curvature is normalised with thermal flame thickness.
- Curvature PDF for case C shows large extent of negative skewness. This negative skewness is there also for cases A and B.

Curvature PDFs (2)

- Creta et al. (Phys. Rev. E 2016) suggested that negative skewness of curvature PDF is a marker for DL (Darrieus-Landau) instability
- The DL instability of a thermo-diffusively neutral flame is most effective in an intermediate range of length scales

Lower limit:
Critical wavelength λ_c

Upper limit:
Nozzle diameter

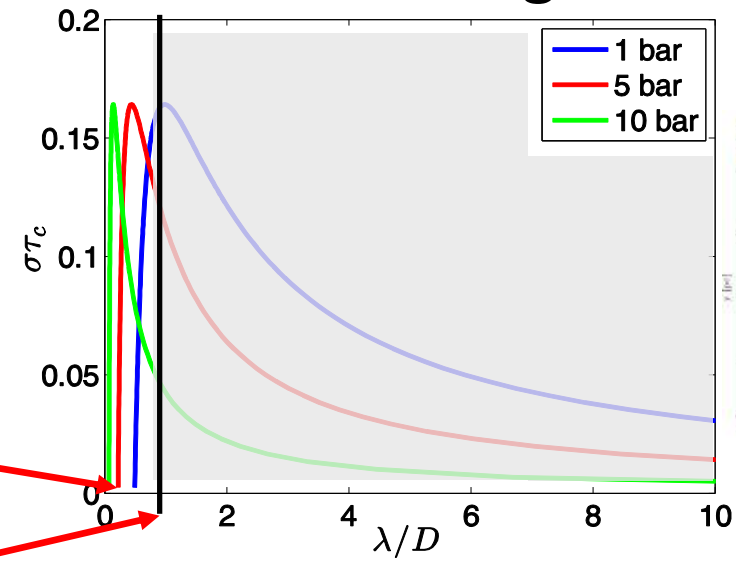

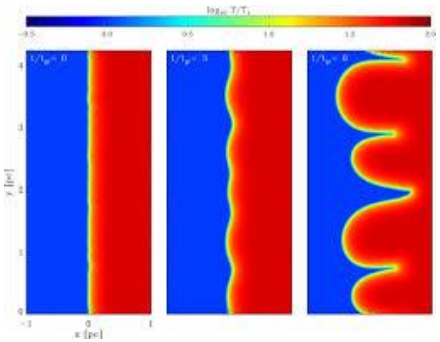

Matalon & Matkowsky (1982 JFM)

Curvature PDFs (3)

- In fact DL instability is promoted for high pressure flames

λ_c/D	P_0	$5P_0$	$10P_0$
Creta & Matalon (JFM 2011)	0.96	0.42	0.3

- Nevertheless DL instability is unlikely to explain the negative skewness for the P_0 flames.
- Huygens principle can be responsible for negative curvature PDF skewness in absence of DL instability

- Solution of G-equation

$$\partial G/\partial t = |\nabla G|$$

Time evolves from red to blue to green.

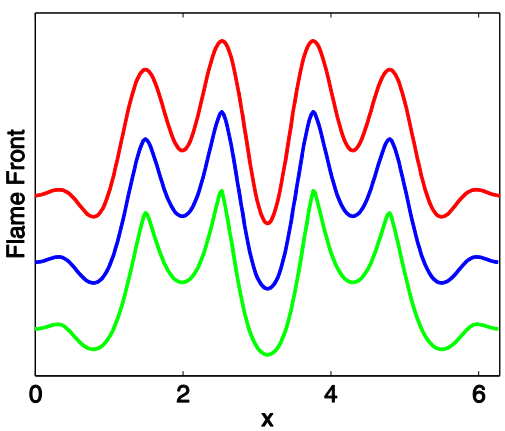

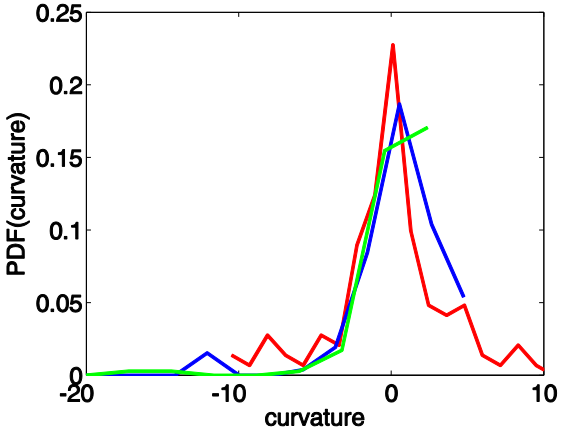

Statistics of S_d/S_L: normalised displacement speed

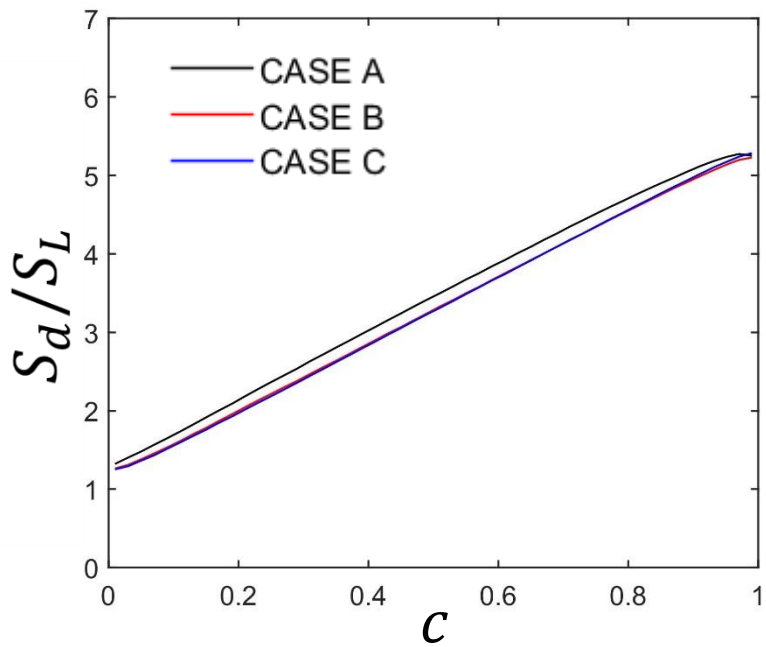

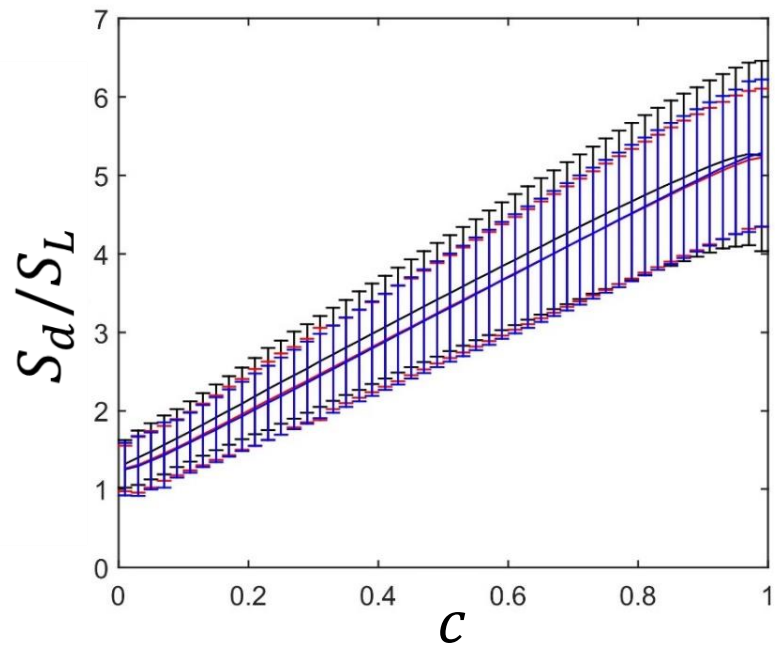

- The standard deviations are shown as bars. Clearly the uncertainly in the difference in the mean value is not significant to draw any meaningful conclusion.
- **No major pressure dependence on the mean normalised displacement speed.**

Statistics of S_d/S_L: normalised displacement speed

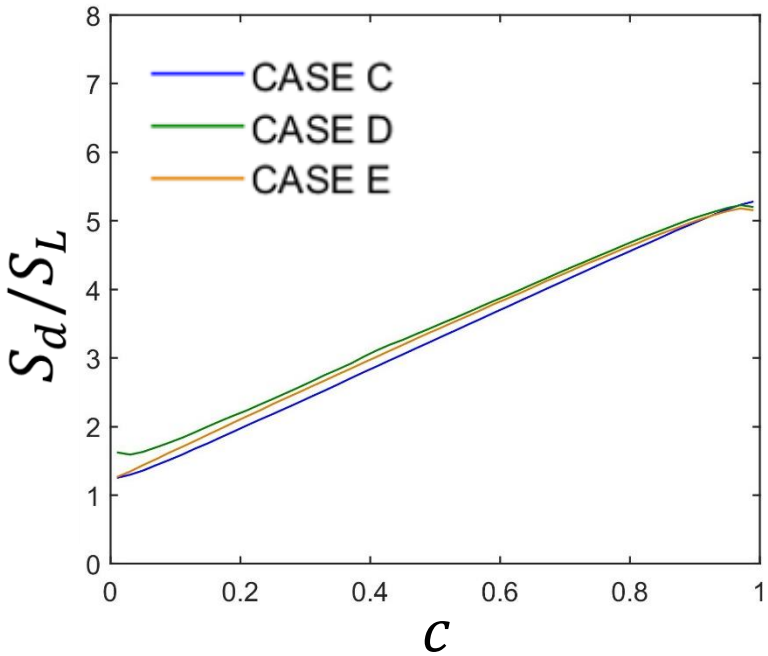

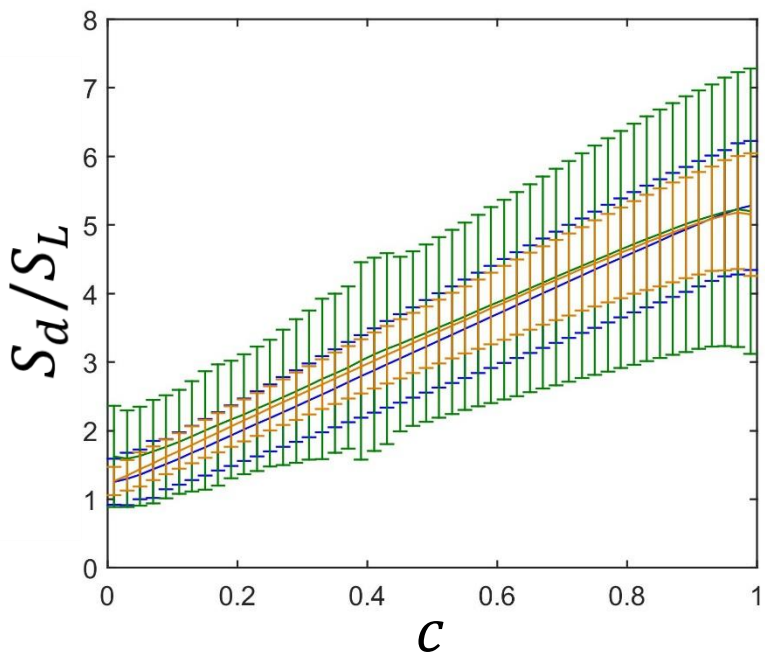

- The standard deviations are shown as bars. Clearly the uncertainly in the difference in the mean value is not significant to draw any meaningful conclusion. Standard deviation increases with increasing u'/S_L.
- **No major u'/S_L and L_{11}/δ_{th} dependences on the mean normalised displacement speed within this parameter range.**

Mean behaviour of S_d/S_L components

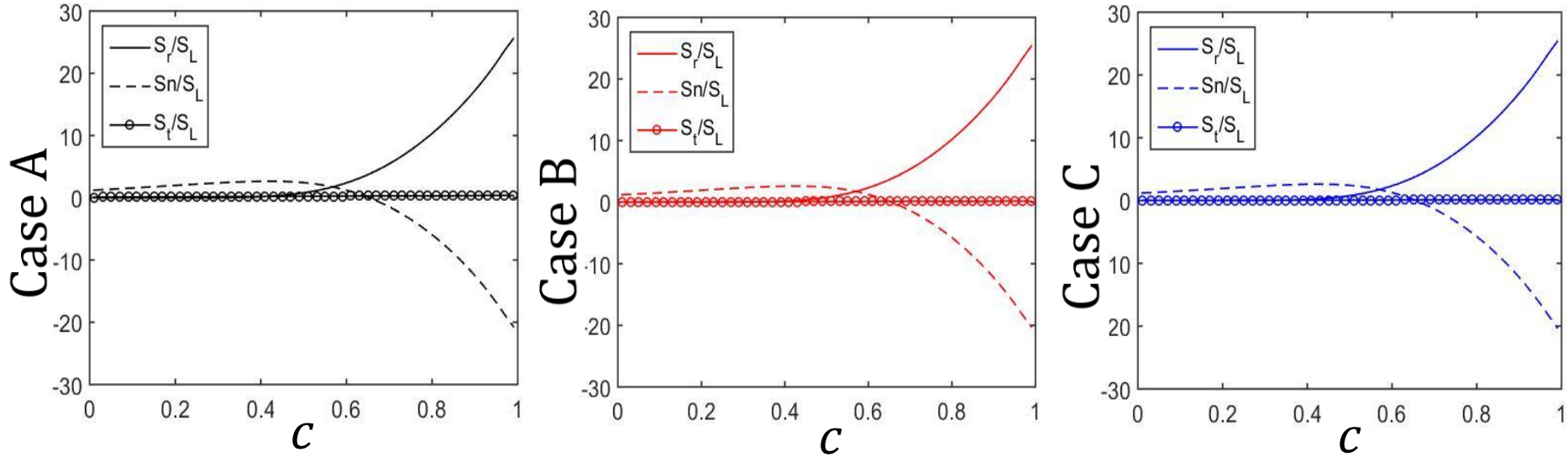

- The mean reaction component of displacement speed S_r/S_L assumes positive values across *c* and increasingly positive toward burned gas.
- The mean normal diffusion component of displacement speed S_n/S_L assumes positive toward unburned gas side but becomes increasingly negative toward burned gas side.
- The normalised tangential diffusion component S_t/S_L dose not contribute significantly to the mean displacement speed but it affects the local variation.

Statistics of $\partial S_\alpha/\partial x_N$ (where $\alpha = d, r, n$, and t)

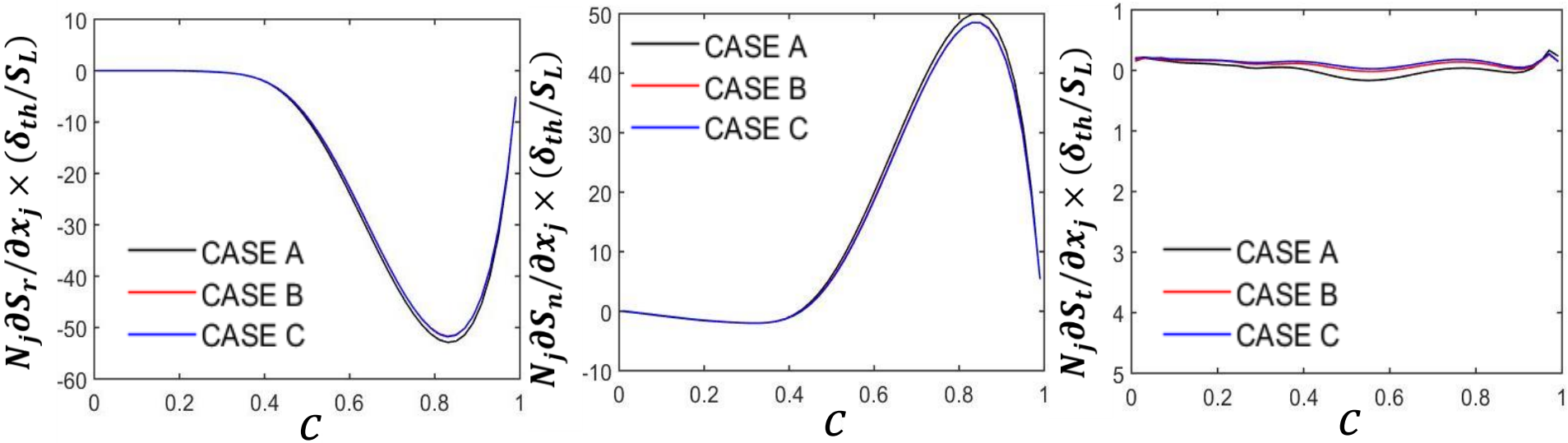

- The contribution of mean $N_j\partial S_r/\partial x_j$ is majorly negative values through the flame, due to S_r/S_L being positive across the flame opposing the flame normal.
- The contribution of mean $N_j\partial S_n/\partial x_j$ exhibits small negative values on the unburned side and increasingly positive toward burned side.
- The mean contribution of $N_j\partial S_t/\partial x_j$ is negligible in comparison to $N_j\partial S_r/\partial x_j$ and $N_j\partial S_n/\partial x_j$.
- The difference in the mean value $[N_j\partial S_\alpha/\partial x_j\ (\alpha = r, n\ \&t)]$is not significant to draw any meaningful conclusion. **No major pressure dependence on the mean normalised added normal strain rate components.**

Statistics of additional normal strain rate $\partial S_d/\partial x_N$

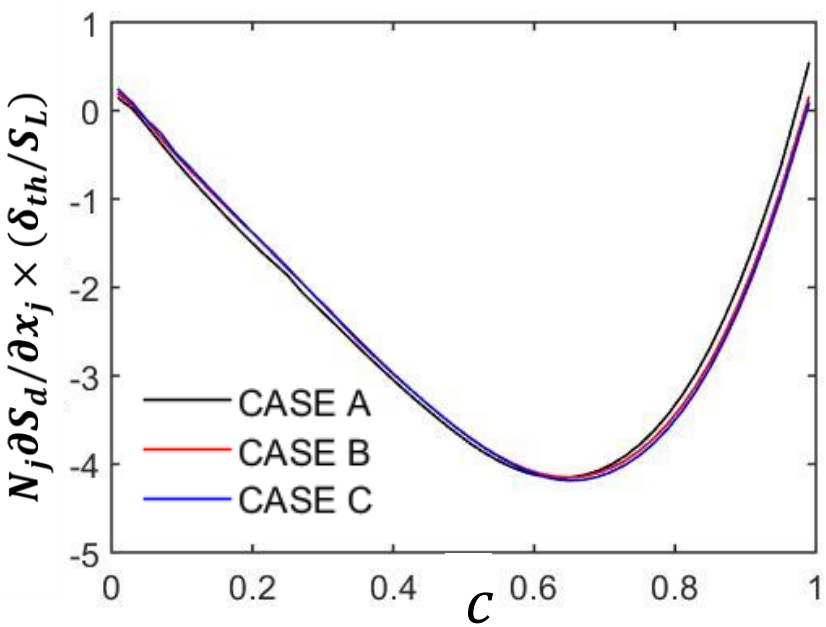

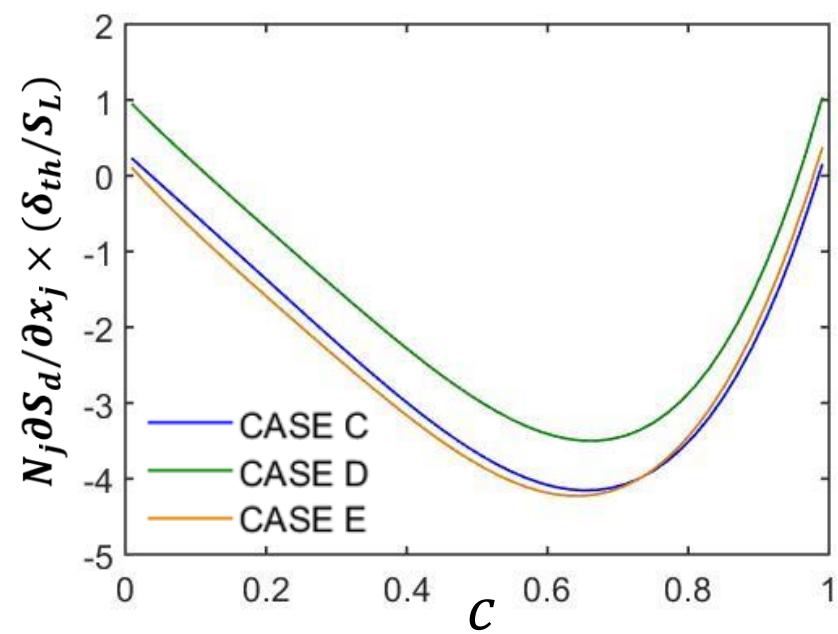

- The mean $N_j\partial S_d/\partial x_j$ remains negative throughout flame.

- The difference in the mean value $N_j\partial S_d/\partial x_j$ is not significant to draw any meaningful conclusion. **No major pressure dependence on the mean added normal strain rate.**

Statistics of $2S_\alpha\kappa_m$ (where $\alpha = d, r + n$, and t)

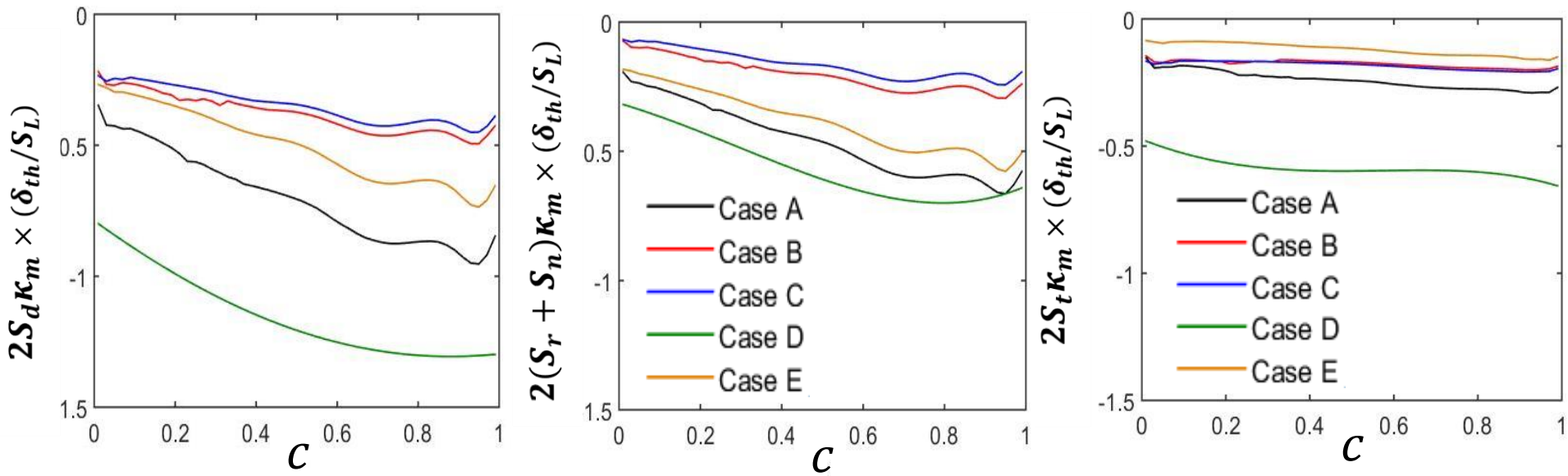

- For the corrugated flamelets regime cases A-C and E the mean behaviour of $2S_d\kappa_m$ is governed by the mean contribution of $2(S_r + S_n)\kappa_m$ where the mean contribution of $2S_t\kappa_m$ remain small.
- The mean contributions of $2(S_r + S_n)\kappa_m$ and $2S_t\kappa_m = -4D\kappa_m^2$ remain comparable for case D representing the thin reactions zone regime of premixed turbulent combustion.
- The magnitude of the mean value of $2S_d\kappa_m$ is the highest for case D and the differences in the mean values of $2S_d\kappa_m$ originate due to the difference in curvature distributions.

Statistics of curvature stretch rate $2S_d\kappa_m$

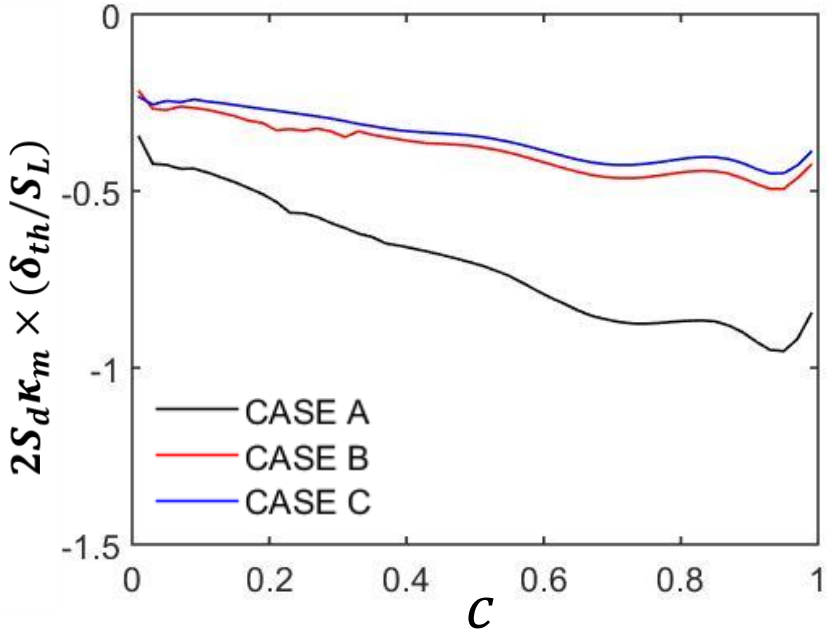

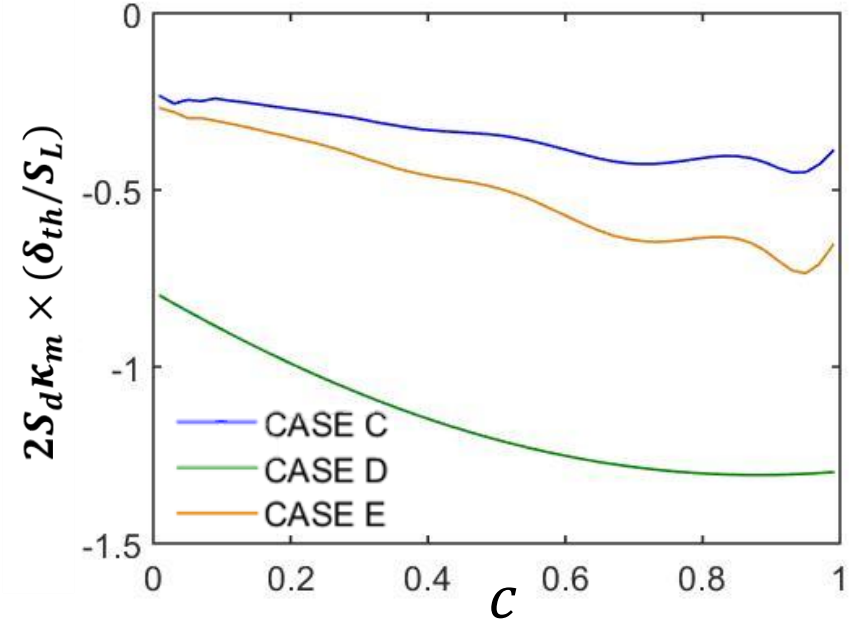

- The mean $2S_d\kappa_m$ remains negative throughout flame.
- The difference in the mean value of $2S_d\kappa_m$ arises due to the difference in curvature distribution and also due to the change in combustion regime.

$a_N^{eff} \times \delta_{th}/S_L$: effective normalised normal strain rate (1)

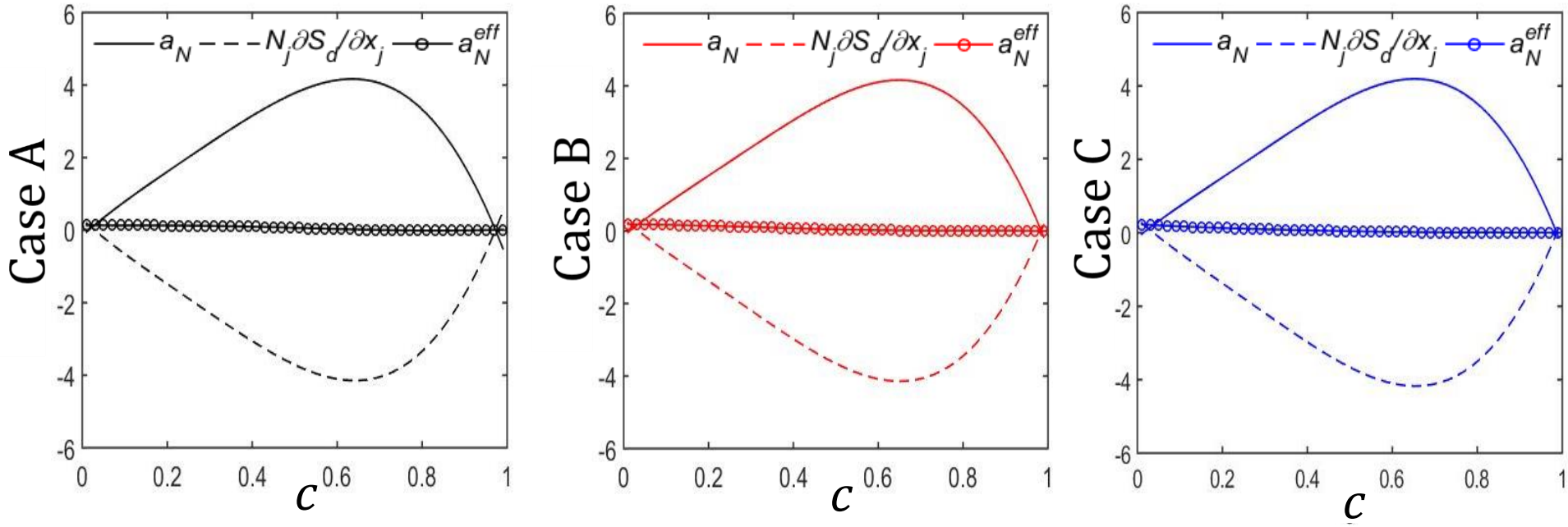

- The magnitude of a_N^{eff} remains small in comparison to the magnitudes of a_N and $N_j \partial S_d / \partial x_j$.
- The mean contributions of a_N and $N_j \partial S_d / \partial x_j$ almost cancel each other.
- **The above behaviour does not seem to be affected by the pressure variation.**

$a_N^{eff} \times \delta_{th}/S_L$: effective normalised normal strain rate (2)

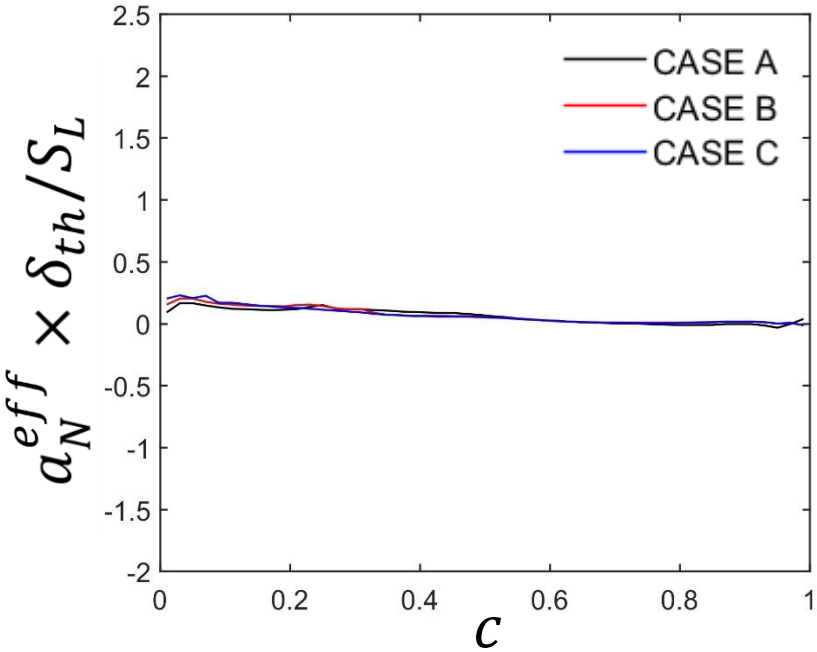

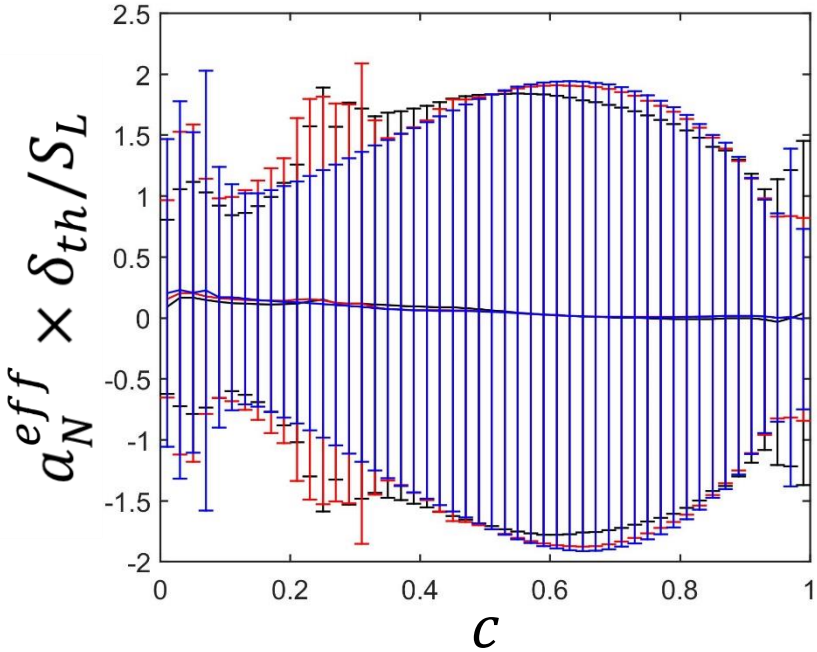

- The standard deviations are shown as bars. Clearly the uncertainly in the difference in the mean value is not significant to draw any meaningful conclusion.
- No difference in effective normal strain rate is reflected in no difference in $|\nabla c| \times \delta_{th}$.
- **No major pressure dependence on the mean normalised effective normal strain rate.**

$a_N^{eff} \times \delta_{th}/S_L$: effective normalised normal strain rate (3)

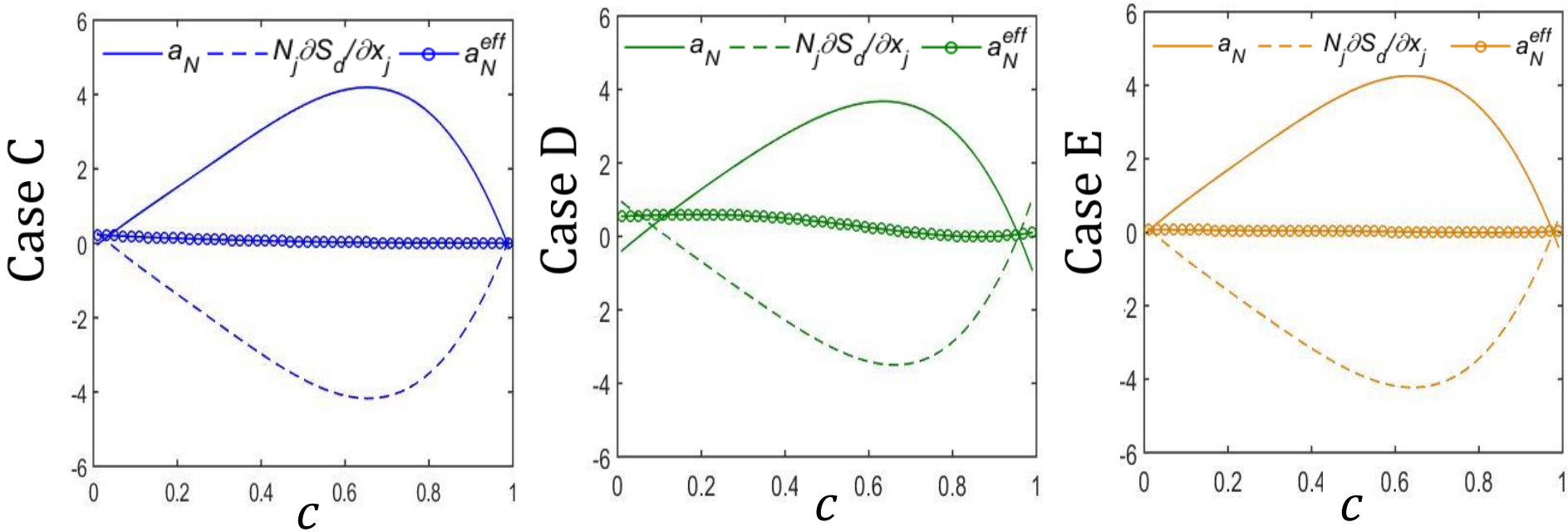

- The magnitude of a_N^{eff} remains small in comparison to the magnitudes of a_N and $N_j \partial S_d/\partial x_j$.
- The mean contributions of a_N and $N_j \partial S_d/\partial x_j$ almost cancel each other.
- **The above behaviour does not seem to be affected by the variation of u'/S_L and L_{11}/δ_{th} within the current parameter range.**

$a_N^{eff} \times \delta_{th}/S_L$: effective normalised normal strain rate (4)

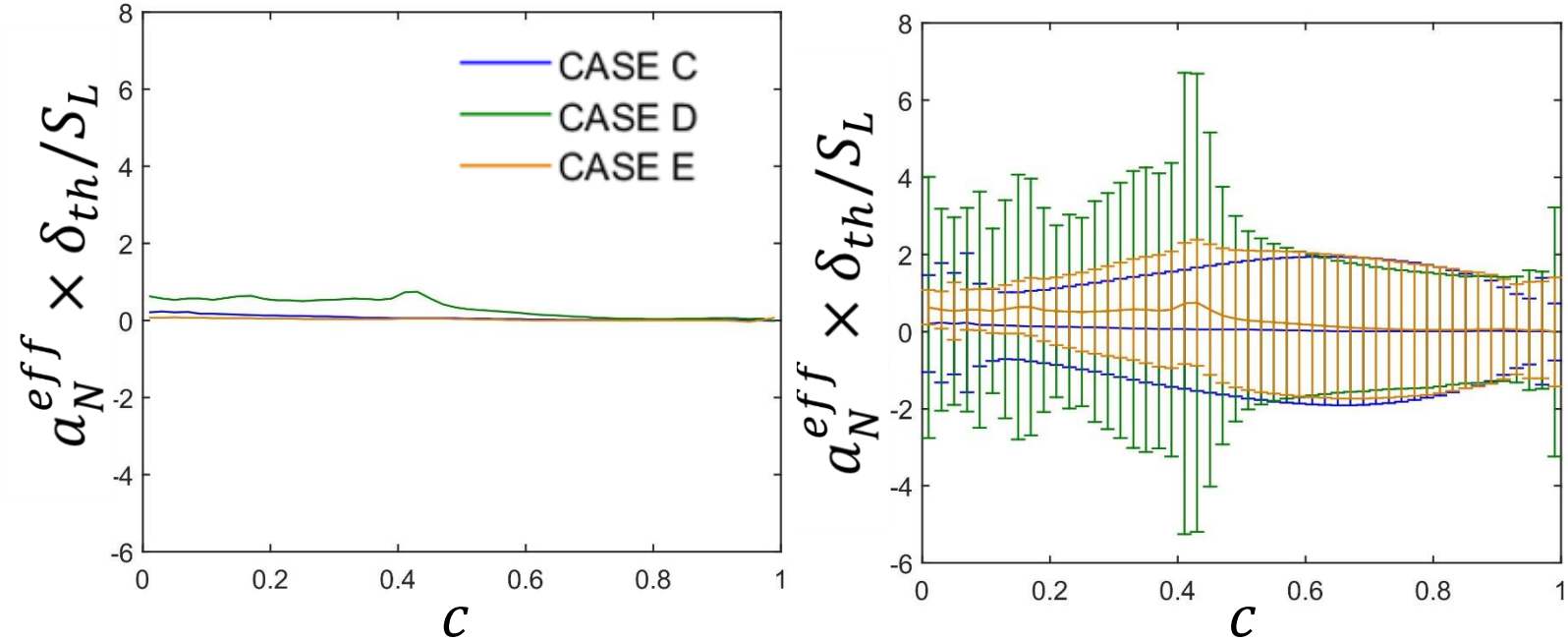

- The standard deviations are shown as bars. Clearly the uncertainly in the difference in the mean value is not significant to draw any meaningful conclusion.
- No difference in effective normal strain rate is reflected in no difference in $|\nabla c| \times \delta_{th}$.
- **No major u'/S_L and L_{11}/δ_{th} dependences on the mean normalised effective normal strain rate.**

$a_T^{eff} \times \delta_{th}/S_L$: effective normalised stretch rate (1)

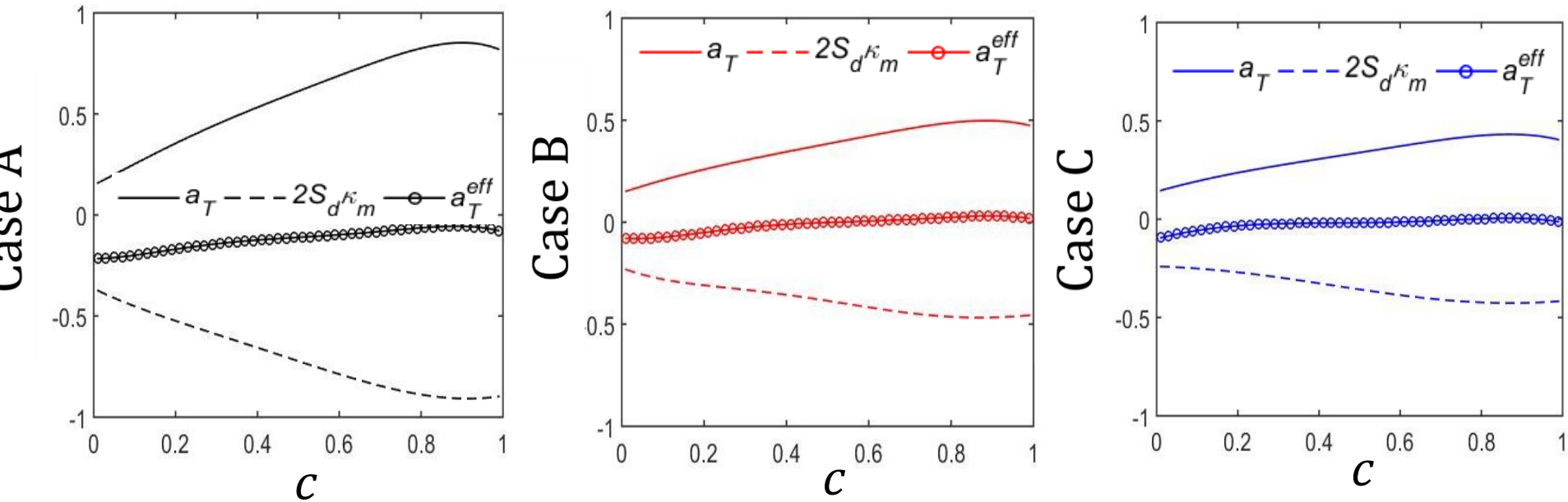

- The magnitude of a_T^{eff} remains small in comparison to the magnitudes of a_T and $2S_d\kappa_m$.
- Although there are differences in the magnitudes of mean values of a_T and $2S_d\kappa_m$, the mean contributions of a_T and $2S_d\kappa_m$ almost cancel each other.
- **Thus, a_T^{eff} does not show a significant pressure dependence for the current parameter range.**

$a_T^{eff} \times \delta_{th}/S_L$: effective normalised stretch rate (2)

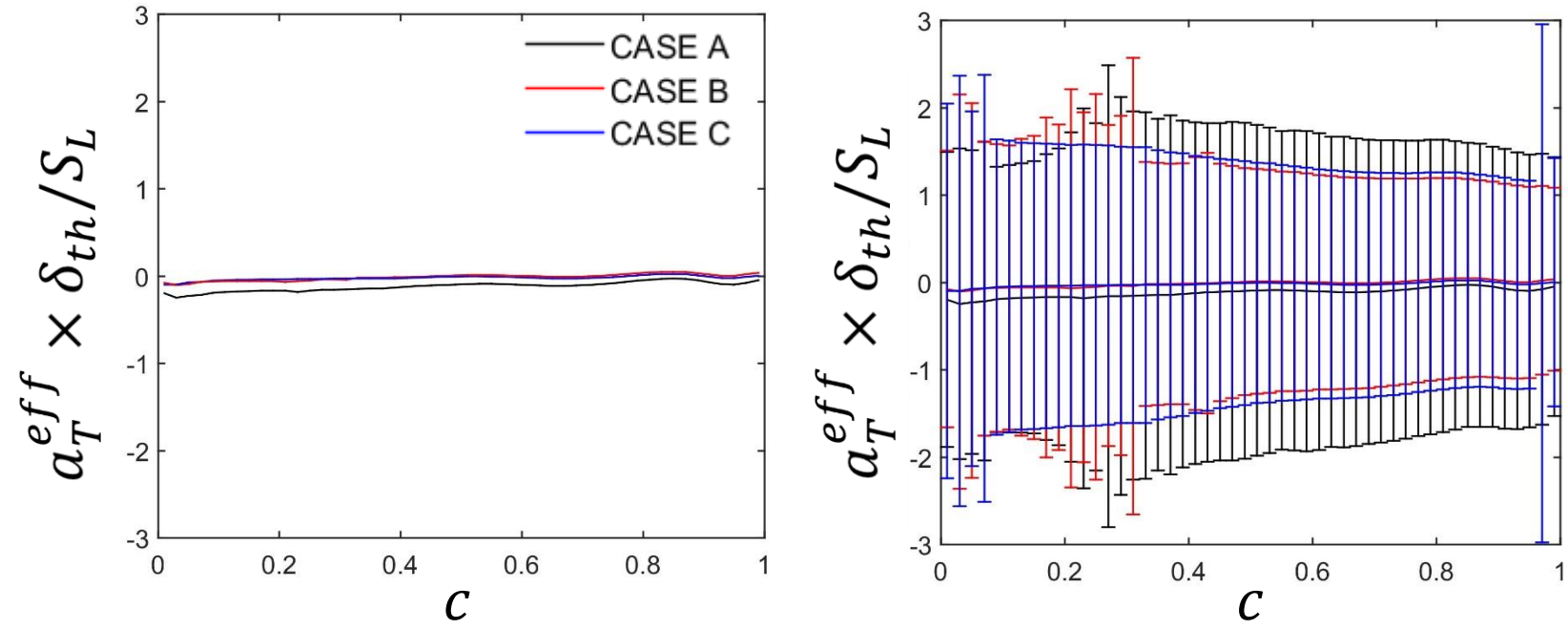

- The standard deviations are shown as bars. Clearly the uncertainly in the difference in the mean value is not significant to draw any meaningful conclusion.
- **No major pressure dependence on the mean normalised effective tangential strain rate within this parameter range.**

$a_T^{eff} \times \delta_{th}/S_L$: effective normalised stretch rate (3)

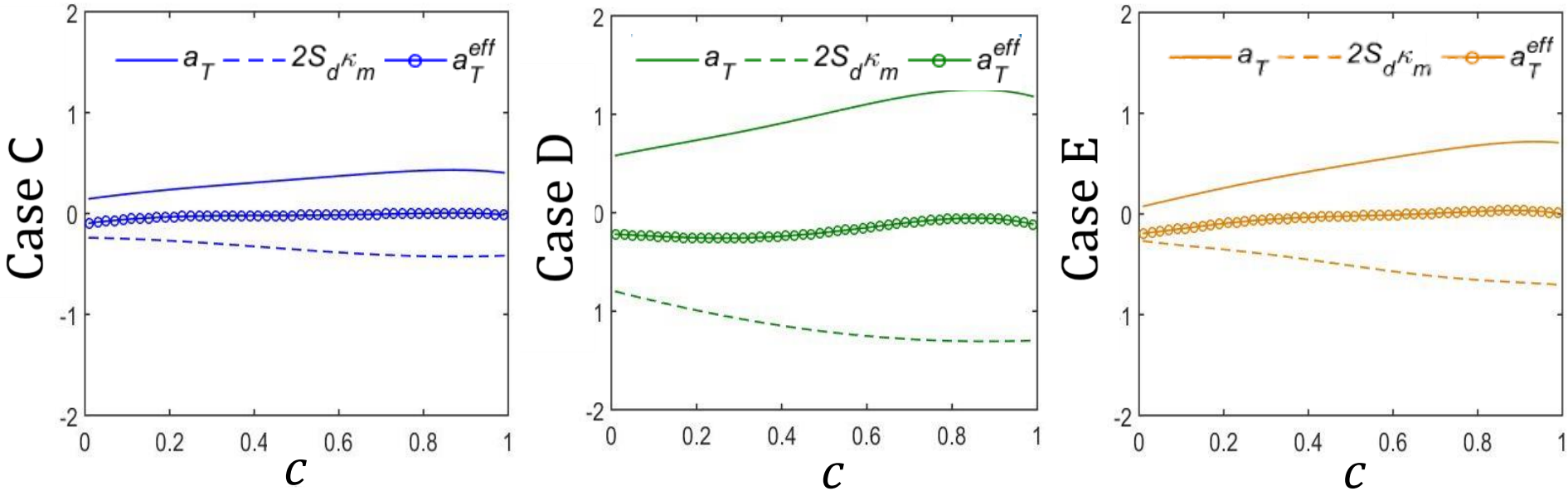

- The magnitude of a_T^{eff} remains small in comparison to the magnitudes of a_T and $2S_d\kappa_m$.
- Although there are differences in the magnitudes of mean values of a_T and $2S_d\kappa_m$, the mean contributions of a_T and $2S_d\kappa_m$ almost cancel each other.
- **Thus, the behaviour of a_T^{eff} does not show significant dependences of u'/S_L and L_{11}/δ_{th} for the current parameter range.**

$a_T^{eff} \times \delta_{th}/S_L$: effective normalised stretch rate (4)

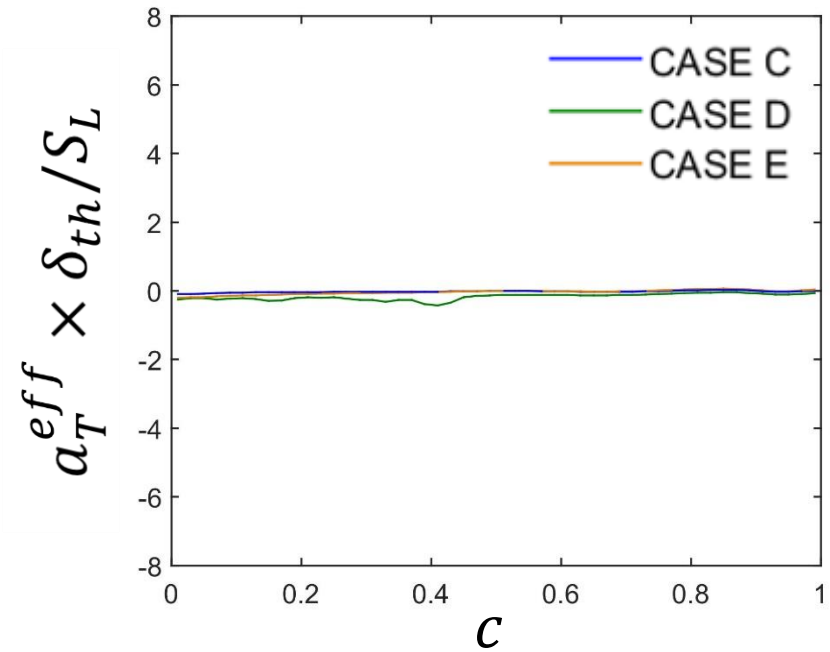

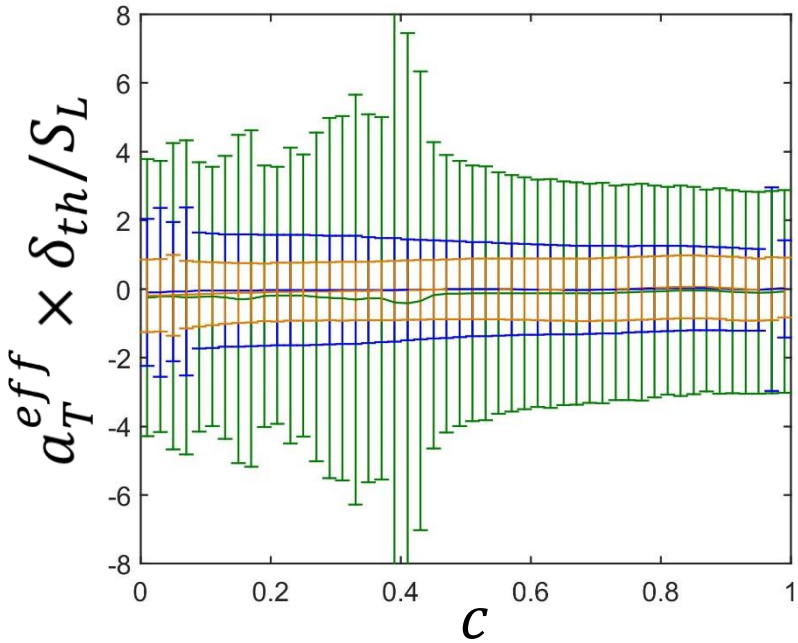

- The standard deviations are shown as bars. Clearly the uncertainly in the difference in the mean value is not significant to draw any meaningful conclusion.
- **No major u'/S_L and L_{11}/δ_{th} dependences on the mean normalised effective tangential strain rate.**

Burning rate and flame area (1)

- The burning rate can be estimated as: $\int_V \dot{\omega} dV$ and it can be presented in the non-dimensional form as:

$$\Omega = [\int_V \dot{\omega} dV]/[\rho_0 S_L D^2]$$

- The flame surface area can be estimated as: $\int_V |\nabla c| dV$ and it can be presented in the non-dimensional form as:

$$\mathrm{A} = [\int_V |\nabla c| dV]/[D^2]$$

Burning rate and flame area (2)

Case	P/P_0	$<\Omega>$	$SD(\Omega)$	$<A>$	$SD(A)$
A	1.0	4.49	0.39	4.15	0.31
B	5.0	4.60	0.42	4.46	0.38
C	10.0	4.60	0.15	4.40	0.14

Case	P/P_0	u'_{inlet}/S_L	L_{11}/δ_{th}	$<\Omega>$	$SD(\Omega)$	$<A>$	$SD(A)$
C	10.0	1.0	15.48	4.60	0.15	4.40	0.14
D	1.0	3.1	4.88	4.53	1.91	4.13	0.43
E	1.0	1.0	15.79	4.10	0.21	3.85	1.63

Here <…> is the mean of realisations and SD (….) is the standard deviation between the realisations

- Appropriate normalisation and pressure scaling lead to collapse of data for different pressure conditions for a given set of values of U_{inlet}/S_L , u'_{inlet}/S_L and L_{11}/D .
- D-L instability at high pressure condition leads to increased flame surface area and burning rate for a given set of values of U_{inlet}/S_L , u'_{inlet}/S_L and L_{11}/δ_{th}.

Conclusions

- Pressure does not seem to have any major impact on the normalised flame thickness and displacement speed at least in the context of simple chemistry. Thus, the models which have been derived and validated for atmospheric pressure are also likely to work for elevated pressures provided correct pressure scalings are used.
- The possibility of having D-L instability is high at elevated pressure conditions. The effects of this instability need to be modelled separately.
- Appropriate normalisation and pressure scaling give rise to collapse of burning rate and flame area for different pressure conditions for a given set of values of U_{inlet}/S_L , u'_{inlet}/S_L and L_{11}/D .
- D-L instability at high pressure condition leads to increased flame area and burning rate for a given set of values of U_{inlet}/S_L , u'_{inlet}/S_L and L_{11}/δ_{th}.

EPSRC

Engineering and Physical Sciences Research Council

N8 Research Partnership | High Performance Computing

lrz Leibniz-Rechenzentrum der Bayerischen Akademie der Wissenschaften

archer

THANK YOU for your attention!